EEG-BASED ASSESSMENT OF CYBERSICKNESS IN A VR ENVIRONMENT AND ADJUSTING STEREOSCOPIC PARAMETERS ACCORDING TO LEVEL OF SICKNESS TO PRESENT A COMFORTABLE VISION

SANAL GERÇEKLİK RAHATSIZLIKLARININ EEG SİNYALLERİ KULLANILARAK BELİRLENMESİ VE RAHATSIZLIK SEVİYESİNE GÖRE KONFORLU BİR SEYİR İÇİN İYİLEŞTİRMELERİN YAPILMASI

UFUK UYAN

ASST. PROF. DR. UFUK ÇELİKCAN

Supervisor

Submitted to

Graduate School of Science and Engineering of Hacettepe University

as a Partial Fulfillment to the Requirements

for the Award of the Degree of Master of Science

in Computer Engineering

2020

DEDICATED

TO MY WIFE AND MY DAUGHTER

WHO SUFFERED MUCH DURING PREPARATION OF

THIS WORK, AND ITS COMPLETION

ABSTRACT

EEG-BASED ASSESSMENT OF CYBERSICKNESS IN A VR ENVIRONMENT AND ADJUSTING STEREOSCOPIC PARAMETERS ACCORDING TO LEVEL OF SICKNESS TO PRESENT A COMFORTABLE VISION

Ufuk UYAN

Master of Science,**Computer Engineering Department**

Supervisor: Asst. Prof. Dr. Ufuk ÇELİKCAN

December 2020, 69 pages

Virtual reality (VR) is an increasingly widespread technology that provides a more realistic and fully immersive experience by using head-mounted displays (HMDs). However, this medium comes with some side effects. Users immersed in a virtual environment (VE) experience motion sickness like discomfort, which is named visually induced motion sickness(VIMS) or, more commonly, cybersickness. In an effort to overcome cybersickness experienced with stereoscopic displays, we propose a novel real-time system to detect cybersickness from the incoming electroencephalogram (EEG) feedback and to mitigate it by updating the cue parameters as per the feedback from the proposed model. The VE used in the study was generated procedurally by tuning levels of 3 different types of cues (navigation speed, scene complexity, and stereoscopic rendering parameters) to induce cybersickness in a varying range of severity. In the first phase of the study, we trained a two-stage shallow convolutional neural network with the EEG data collected from the users while immersed in the VE. The proposed two-stage model was utilized to detect cybersickness and to classify factors causing cybersickness, respectively. The performance of the cybersickness detection

model reached an overall accuracy of 76.26%, while the factor type classification model achieved 81.01% overall accuracy. To assess the performance of the proposed cybersickness detection and mitigation system, an experiment consisting of two control sessions, and one models-in-the-loop session (MIL) was conducted in the second phase of the study with a different user sample. The differences in the Simulator Sickness Questionnaire (SSQ) responses collected before and after each session, and the time-dependent changes in the cue parameters showed that the participants felt less cybersickness during the MIL session in which the proposed cybersickness detection and mitigation system (CDMS) was utilized.

Keywords: Cybersickness, Virtual Reality, Visually Induced Motion Sickness, EEG-based Cybersickness Detection, Deep Learning, Cybersickness Mitigation

ÖZET

SANAL GERÇEKLİK RAHATSIZLIKLARININ EEG SİNYALLERİ KULLANILARAK BELİRLENMESİ VE RAHATSIZLIK SEVİYESİNE GÖRE KONFORLU BİR SEYİR İÇİN İYİLEŞTİRMELERİN YAPILMASI

Ufuk UYAN

Yüksek Lisans, Bilgisayar Mühendisliği

Danışman: Dr. Öğretim Üyesi Ufuk ÇELİKCAN

Aralık 2020, 69 sayfa

Sanal gerçeklik (VR), başa takılan ekranların (HMD) kullanılmasıyla daha gerçekçi ve sürükleyici bir deneyim sağlayan, giderek yaygınlaşan bir teknolojidir. Fakat, bu teknolojik gelişim bazı yan etkileri beraberinde getirmektedir. Sanal bir ortamı deneyimleyen kullanıcılar hareket tutması rahatsızlığına benzer rahatsızlık yaşarlar. Sanal ortamlara maruziyet sonrasında deneyimlenen bu rahatsızlık gerçek bir fiziksel hareketin olmaması nedeniyle sanal gerçeklik tutması (cybersickness) olarak adlandırılmıştır. Bu çalışmada amacımız sanal ortamlarda deneyimlenen sanal gerçeklik tutması rahatsızlığını tespit etmek, sınıflandırmak ve bu rahatsızlığı hafifletmek için ilgili sahne parametrelerini güncellemektir. Sunulan sanal ortamda kullanıcıların rahatsızlığa maruz kalabilmeleri için sanal ortamlar oluşturulurken navigasyon hızı, sahne karmaşıklığı ve stereoskopik sahne oluşturma parametreleri kullanılmıştır. Sunulan sanal ortamı deneyimleyen katılımcılardan eşzamanlı olarak toplanan elektroensefalogram (EEG) verileri, Filtre Bankası Ortak Mekansal Patern (FBCSP) algoritmasına dayanan iki aşamalı sığ evrişimli sinir ağını (Shallow Convolutional Neural Network) eğitmek için

kullanılmıştır. Önerilen iki aşamalı model, sanal gerçeklik tutması rahatsızlığını tespit etmek ve bu rahatsızlığa neden olan faktörü sınıflandırmak için kullanılmıştır. Önerilen modelde rahatsızlığın tespit performansı %76.26'lik doğruluğa ulaşırken, rahatsızlığa neden olan faktörün sınıflandırıldığı modelde %81.01'lik doğruluk performansı elde edilmiştir. Önerilen sistemin gerçek zamanlı performansını değerlendirmek için, farklı katılımcılar ile iki kontrol oturumundan ve bir modellerin döngüde olduğu oturumdan oluşan bir deney gerçekleştirilmiştir. Her bir oturumun başında ve sonunda uygulanan Simülatör Rahatsızlığı Anketi (SSQ) puanlarındaki farklar ve sahne parametrelerindeki zamana bağlı değişimler, katılımcıların önerilen sanal gerçeklik tutması tespit ve azaltma sisteminin (CDMS) kullanıldığı oturumda daha az rahatsızlık deneyimlediklerini göstermiştir.

Anahtar Kelimeler: Sanal Gerçeklik Tutması, Sanal Gerçeklik, EEG Tabanlı Rahatsızlık Tespiti, Sanal Gerçeklik Tutması Hafifletme, Derin Öğrenme

ACKNOWLEDGEMENTS

First and foremost, I would like to thank to my supervisors Asst. Prof. Dr. Ufuk Çelikcan for his valuable advice and guidance. At every stage of this thesis, he supported me with his knowledge, experiences, motivations and encouragements.

Besides I would like to thank to my thesis committee members, Prof. Dr. Haşmet GÜRÇAY, Assoc. Prof. Dr. Mehmet Erkut ERDEM, Asst. Prof. Dr. Serdar ARITAN and Asst. Prof. Dr. Abdullah BÜLBÜL for reviewing this thesis and giving insightful comments.

I would like to express my sincere gratitude to ASELSAN, Inc. for allowing me to attend classes and get a master's degree despite the intensity of the works. I would also thank to my teammates Dr. Kenan AHISKA and Ali DOĞAN for their suggestions and support.

I would also thank to members of Hacettepe Univesity Computer Vision Laboratory(HUCVL) and Alper ÖZKAN for his consistent support.

Finally, I am deeply grateful to my parents for believing in me throughout my educational life. They always support and encourage me with their best wishes.

CONTENTS

Page

FIGURES

Page

TABLES

Chapter 1.

INTRODUCTION

Virtual reality (VR) technologies, which were first used in military simulation and training applications, have been employed in many fields, especially education, entertainment, health, and games, as a result of enriched virtual contents and affordable prices. All the digital and physical elements that enable users to feel and interact as if they are really in a virtual world are called VR.

Various display technologies are employed in modern VR systems, including the head-mounted display (HMD), reality theater, and computer-assisted VE (CAVE). Today, the HMD-based setups are the most commonly used ones since they are more affordable, meet high mobility requirement, and provide participants with a full immersion experience in which a user is wholly detached from the reality.

Despite the recent breakthroughs in VR technologies, users immersed in virtual environments (VEs) with modern VR setups are still prone to experience cybersickness. According to the prior studies, 30% [6] to 80% [7] of users immersed in a VE are affected by this ailment. Its symptoms, including nausea, cold sweats, dizziness, headache, increased salivation, and fatigue, are similar to those of motion sickness. Identifying cybersickness is not straightforward, as it contains many symptoms, and these symptoms vary from person to person. Hardware limitations, such as lag, tracking accuracy, and flicker, were once considered the primary sources of discomfort felt in VEs [8]. Even though these hardware-related limitations have been reduced considerably, the sickness experienced remains to be the most notorious aspect associated with VR [9].

While there is no consensus on the biological causes of cybersickness [10], hypotheses have been proposed, and experiments have been conducted about the factors that may trigger its onset. The visual-vestibular conflict (VVC) is widely seen as the leading cause of cybersickness based on the assumption that the external stimulus is perceived differently with visual and vestibular senses [11]. Cybersickness is mainly induced when translational and rotational movement in a VE are exaggerated and the resulting perceived motion is not felt by the viewer's vestibular system. Furthermore, visual motion perception in a VE is affected by scene complexity [12].

Another prevailing cause is the vergence accommodation conflict (VAC). This conflict occurs when there is a mismatch between the perceived depth of a virtual 3D object and the focusing distance of the eyes [13]. In stereoscopic VR headsets, a focused virtual object is displayed on the head-mounted-display (HMD), which is at a fixed depth away from eyes, but the perceived depth of the object varies with scene content [14]. In real life, the depth for accommodation and vergence are same. Although people have a degree of tolerance against this conflict, it can contribute to focusing problems, visual fatigue, and eyestrain with long term use, especially if the depth perception is exaggerated.

There are three commonly used methods to detect and grade cybersickness. The primary method is using questionnaires. Since cybersickness has similar symptoms with motion and simulator sickness, the Simulator Sickness Questionnaire (SSQ), which was proposed by Kennedy et al [15], is utilized in cybersickness studies. It takes a long time to complete the SSQ, and it is considered that the discomfort to be measured may decrease during the filling out period. Therefore, in this study, a single-question discomfort query, which takes less time, was used for grading the general discomfort level during exposure to a VE. Another method used to detect cybersickness is measuring postural instability. The assumption that cybersickness causes postural imbalance is taken into consideration in this method. Unlike the questionnaire method, immersion is not interrupted, and the user is not disturbed for measurement. Generally, sensors connected to the body or systems containing more than one camera are utilized to measure postural instability. Lastly, the severity of visual discomfort is graded using bio-signals collected from participants. Thanks to the developing sensor technologies, the physiological state of the body can be easily measured using a variety of bio-signals. Bio-signals such as an electrocardiogram (ECG), blood pressure, electrogastrogram (EGG), respiration (RSP), electroencephalograms (EEG), skin temperature are used to

detect cybersickness experienced in VEs. In this study, EEG signals were used to measure the cybersickness.

Electroencephalography (EEG) is a method used to evaluate electrical activities and functions in the brain. The EEG signals collected through the electrodes that come into contact with the scalp have to be preprocessed before use because they have a low signal to noise ratio (SNR), vary from person to person and are non-stationary which may cause the trained model to predict different results even when the model is tested in the user to whom the model is trained. Preprocessed EEG signals are generally represented by a few relevant features which describe the task-related information by proper feature extraction method. Preprocessing and feature extraction methods require expertise as they differ according to the application. Deep learning algorithms have achieved cutting-edge performance in areas such as computer vision and natural language processing (NLP), thereby significantly reducing the need for manual feature extraction.

Current approaches to detecting and mitigating cybersickness generally do not go beyond the scope of binary classification of cybersickness experienced in a virtual environment and post-processing of the scenes presented in line with the results obtained. There is no study in which cybersickness is detected and mitigated in real time, except for the study in which the field of view(FOV) is narrowed and the user is given a voice command to reduce the navigation speed [16]. In line with the increasing demand for an objective cybersickness evaluation and a real-time mitigation technology, we explore the factors of navigation speed, scene complexity, and stereoscopic rendering parameters, which are (camera) inter-axial distance and (camera) convergence distance, to gain greater insight into cybersickness experienced in a VE. For a more objective cybersickness assessment, we utilize electroencephalogram (EEG) signals collected from the users.

Our main contributions in this study include:

- simulating various levels of the navigation speed, scene complexity, and stereoscopic rendering parameters by isolating from each other to induce cybersickness,
- a neural network model for detecting and classifying factors causing cybersickness with EEG data collected from user,
- a real-time, online mitigation of experienced cybersickness by tuning the cue parameters following the feedback from the proposed model,

- satisfactory performance without the need for individual calibration.

The remainder of this dissertation proceeds as follows. Chapter 2 gives an overview of the related works and introduces the basic principles and terminologies used in this study. Chapter 3 describes our methodology, where experimental setup and the architecture of neural network models are detailed. Chapter 4 presents the results for the both model training and feedback phase experiment. Finally, a discussion of the results and a conclusion are given in Chapter 5.

Chapter 2.

RELATED WORKS AND BACKGROUND

2.1. Related Works

The detection of cybersickness experienced in a virtual environment (VE) with electroencephalogram data using deep learning algorithms is a subject that has recently been investigated. Since there are not enough studies in the literature about this topic, we carried out the literature review under four subtitles within the context of this study. Firstly, we reviewed studies on cybersickness and examined the factors that caused visual discomfort. Afterward, we examined studies in which cybersickness was detected with traditional approaches using bio-signals and investigated the features used in the detection. Moreover, studies in which task-related information was decoded through deep learning algorithms using EEG data were reviewed. The relationship between the architectures of the deep learning algorithms and the activity intended to be detected was investigated. Besides, before feeding on proposed algorithms, the preprocessing steps applied to the time-series EEG data were examined. Lastly, we investigated studies in which the EEG signals were decoded to detect cybersickness experienced in a VE by using deep learning algorithms.

Cybersickness research has gained more importance in recent years as the use of virtual and augmented reality systems has shifted from experienced users to general users. Rebenitsch

et al. [10] published a comprehensive review of cybersickness. In this review, possible factors considered to cause cybersickness were compared and measurement methods used to determine the severity of symptoms were investigated. Kolasinski et al. [17] proposed over 40 possible cybersickness factors, which were categorized as simulator, task, and individual factors. Individual factors include all personal factors, especially age, gender, physical and mental characteristics, and VR experiences. Arns et al. [18] investigated that younger participants(under the age of 15) were less likely to experience cybersickness than older ones. The study of Park et al. [19] supported this finding by showing that the withdrawal rates of the young participants during the experiments were lower than the old participants. Numerous studies have been conducted to investigate the correlation between visual discomfort induced in VEs and gender. Although some studies have shown that females are more susceptible to cybersickness than males, in some studies, there was no statistical correlation between gender and cybersickness [20]. Hill et al. [21] demonstrated that the severity of the symptoms of cybersickness decreased through habituation. However, there is no consensus on how long this habituation effect will last. Howarth et al. [22] conducted an experiment including ten sessions, one week between each session, and half of the participants showed no symptoms at the end of the experiment. Another critical factor investigated in cybersickness studies is the immersion duration in a VE. Stanney et al. [23] showed that an increase in exposure time caused an increase in the severity of cybersickness related symptoms. In the experiment carried out, 20% of the participants could not complete the 60-minutes session. Half of these participants withdrew before the first 20 minutes of the experiment.

Several studies focused on the effects of hardware configuration and rendering techniques related factors on cybersickness. Sharples et al. [24] compared the effect of display types on the severity of experienced cybersickness. According to the reported results, the head-mounted display causes a higher SSQ-Nausea score than other types of display. Yildirim [25] investigated the effect of the display type on severity of cybersickness and reported that while HMDs induce significantly more discomfort than flat displays during gameplay. Somrak et al. [26] examined the effect of various HMDs and a 2D TV on cybersickness and found similar results, that is, HMDs induced more discomfort than the 2D TV. The broader field of view in VEs increases the sense of presence. Many studies have been conducted to ascertain the correlation between the visual field of view and cybersickness severity. Seay et al. [27] and Duh et al. [28] immersed participants in VEs with various fields of view and reported that the increase in the field of view caused an increase in visual discomfort.

A large part of the research regarding cybersickness is on the effects of software and simulation related factors. Cybersickness is a form of motion sickness that is triggered by visual stimuli in immersive virtual environments. The correlation between the navigation speed in a VE and the severity of cybersickness related symptoms is extensively investigated. So et al. [29] reported that an increasing navigation speed consistently increases the severity of motion sickness. The navigation speed in a VE correlated with cybersickness, but its limits have not been firmly defined. The blur effect that occurs when navigation reaches high speeds is considered to reduce the cybersickness experienced. Wibirama et al. [30] examined the effect of fixation points on cybersickness and reported higher intensity of cybersickness with the higher speed footage of a real roller coaster rather than the slower computer-generated path. Keshavarz et al. [31] reported that the intensity of vection on users was connected to their speed and also affected by the crowdedness of the scene. Scene content may also affect cybersickness, but the correlation between scene content and cybersickness is less certain. Welch et al. [32] claimed that increased visual realism in the VE strengthens the sense of presence. However, Jaeger et al. [33] pointed out that an increase in the detail level of the scene content caused an increase in SSQ scores. So et al. [29] conducted an experiment in which participants were immersed in a VE at three different complexity levels achieved by changing the texture of the mappings. The results unveiled that an increase in the level of details caused an increase in total SSQ scores. Terenzi et al. [34] investigated user reactions to different particle fields with varying acceleration and optic flow type and found that there are different thresholds of discomfort relating to different flow fields.

Mom-Williams et al. [9] investigated the effect of the stereoscopic depth in a virtual environment on the visual discomfort and reported that shifting convergence distance may increase heterophoria. The camera separation directly affects the amount of depth perceived in a VE and should be aligned with the user's interpupillary distance. Kolasinski et al. [35] investigated that cybersickness related symptoms become more severe when participant's eyes separation, and the spacing between the virtual cameras differs more. Howarth et al. [36] tested the sesitivity of heterophoria to the inter-axial distance and reported that the experienced cybersickness was mitigated by the alignment between the user's interpupillary distance and camera inter-axial distance. It has been revealed in the cited articles [29, 31, 33] that navigation speed, scene complexity and stereoscopic rendering parameters have a direct effect on cybersickness. In the light of these findings, the factors mentioned were isolated from each other and used to induce cybersickness.

The detection of cybersickness using bio-signals has been studied thoroughly. Kim et al. [7] investigated the correlation between exposure duration in a VE and cybersickness by using bio-signals of EEG, eye blink rate, heart rate, gastric tachyarrhythmia, skin conductance, and respiration rate. The results confirmed that cybersickness had a significant correlation with gastric tachyarrhythmia, eye blink rate, heart period, and EEG delta and beta waves. In another study, Kim et al. [16] proposed a real-time and artificial neural network based cybersickness detection system whose inputs were bio-signals collected from participants exposed to a VE. Electrocardiogram, electrooculogram, skin conductance, skin temperature, photoplethysmogram, electrogastrogram, respiration, and electroencephalogram (EEG) signals were utilized to detect cybersickness during immersion. The proposed system provided a narrow field of view and voice feedback suggesting to reduce navigation speed after the detection of visual discomfort. Results indicated that SSQ scores significantly decreased with the help of the proposed cybersickness relief system. Chang et al. [37] found that alpha and beta band power attenuated when participants were exposed to a VE. Chen et al. [38] investigated the effect of motion sickness with the EEG signals using a car simulator and found that alpha power attenuated in the parietal and motor areas while theta and delta band power augmented in the occipital area. Kang et al. [39] suggested a wellness platform to classify visual discomfort induced in a stereoscopic 3D environment by using a support vector machine algorithm. Participants were immersed in five different VEs created with random-dot stereogram (RDS), where a similar object was presented at different depth levels. As a result, the overall average log spectra of EEG data attenuated following the increase in disparity level within binocular fusion limit of participants. This study formed the basis for our work on real-time detection and mitigation of cybersickness using EEG signals. However, since cybersickness is triggered by multiple factors in current HMD-based stereoscopic environments, this study is insufficient to meet the needs. Kevric et al. [40] compared the empirical mode, the discrete wavelet transform, and the wavelet packet signal decomposition methods in terms of classification performance of two classes motor imagery task with EEG data. The results unveiled that the wavelet packet decomposition method with applying multiscale Principal Component Analysis (PCA) for the noise elimination algorithm reached up to an accuracy of 92.8%. Considering the price, safety, mobility, and the need for not disturbing the vision, EEG emerges as one of the most promising types of bio-feedback to evaluate cybersickness objectively in the light of recent technological advances.

Deep learning algorithms show superior performance in the classification of numerous complex data, especially in computer vision and natural language processing, due to its robust

feature extraction capability. BBecause EEG data has a low signal to noise ratio and the reaction of brain to stimuli may be different, it is necessary to apply proper preprocessing actions and to extract the explanatory features in order to decode the task-related information. Deep learning algorithms make it possible to learn from raw time-series EEG data by extracting the multiple levels of features necessary for accurate classification without being an expert in EEG signal processing. Kuang et al. [41] proposed a deep belief network for the classification of motor imagery tasks with raw EEG data. The classification accuracy of the proposed algorithm exhibited better performance than the support vector machine approach. Rezaeitabar et al. [42] investigated the classification performance of motor imagery tasks with convolutional neural networks (CNN), stacked auto-encoders (SAE), and combined CNN-SAE. The combined CNN-SAE method provided better performance over state of the art approaches in the dataset IIb from BCI Competition IV and the dataset II from BCI Competition II. Wilaiprasitporn et al. [43] proposed cascaded CNN-LSTM and CNN-GRU networks to extract both spatial and temporal information from raw EEG data for person identification. The person recognition performances of both proposed methods were analyzed for EEG signals collected from 32 electrodes on the entire scalp. While both methods achieved higher accuracy compared to SVM, CNN-GRU performed better than CNN-LSTM in terms of short training time and accuracy performance.

Yang et al. [44] suggested a CNN to classify emotional state. The experimental results showed that the proposed method reached up to 90.24% and 89.45% classification accuracies for arousal and valence states, respectively. Schirrmeister et al. [5] proposed neural networks in architectures with different number of convolution layers to classify motor imagery by using time series EEG signals as input. The first architecture is a shallow network with two convolution layers and structurally models the Filter Bank Common Spatial Pattern (FBCSP) algorithm, the winner of the BCI competition IV 2a and 2b [45]. To extract a variety of task-related features, another deep learning architecture with five convolution layers was also proposed. The performances of the proposed models were measured by comparing them with the actual FBCSP algorithm. The results unveiled that both models provided better classification accuracy in the motor imagery task than FBCSP. Zhang et al. [46] introduced parallel and cascaded recurrent CNN architectures. The time-series EEG data was first converted into a 2-dimensional form, which is mapped according to the position of the electrodes, and fed into the proposed models by taking the time sampling with the sliding window method. The results demonstrated that both of the proposed methods performed better than the state-of-art methods in decoding the task-related information. Bashivan et

al. [47] proposed a novel deep learning approach to classify cognitive load. In the suggested model, it is aimed to extract the temporal, spatial, and spectral features by using CNN and LSTM networks in combination. EEG data is divided into equal chunks for each trial before being used as an input. Afterward, spectral power was calculated in theta, alpha, and beta bands for each channel. The topology-preserving azimuthal equidistant projection was applied to transform the location of the electrodes on the scalp to a 2D image. The classification error of 15.3%, which achieved in the state of art method, was reduced to 8.9%. Lawhern et al. [4] introduced a single CNN architecture to classify both event related potential (ERP) and oscillatory-based brain computer interfaces (BCI) named EEGNet. The classification performance of the proposed CNN architecture was evaluated on the EEG datasets from four widely used BCI paradigms. The results demonstrated that EEGNet performs better than classical approaches when a limited number of training data is available.

Jeong et al. [48] investigated the cybersickness classification performances of the CNN and DNN. The CNN provided better performance over DNN, but DNN was better concerning the computational cost. Kim et al. [49] proposed a novel two-stage cybersickness level predictor. In the first stage, CNN based EEG spectrogram encoder was utilized to estimate the cognitive state. The estimated cognitive state was combined with the extracted features of the second stage, which consists of a combined CNN-RNN based VR video sequence encoder to predict cybersickness level. The proposed model was tested using the ETRI-VR database, and accuracy of 89% was achieved.

Current approaches for detecting and mitigating cybersickness generally do not go beyond the scope of binary classification of cybersickness experienced in a VE and post-processing of the scenes presented in line with the results obtained. There is no study in which cybersickness is detected and mitigated in real-time, except for the study in which FOV is narrowed and the user is given a voice command to reduce the navigation speed [16].

2.2. Background

In this section, I summarize the basic information about virtual reality, stereoscopic vision, cybersickness, and EEG signals.

2.2.1 Virtual Reality

Technically, the term virtual reality is used for computer-based 3D environments where individuals experience the feeling of presence. Although the virtual reality technologies have become more popular with the invention of head-mounted displays (HMD), studies in this area go back decades. The first modern virtual reality application is a multi-sensor simulator called "Sensorama" developed by Morton Heiling in 1962. With this prototype, a motorcycle experience in New York city is simulated as if it were in the real world. Later, virtual reality applications started to be developed for military purposes and were used by the USA as a training tool to increase soldiers' operational experience. Nowadays, the size of VR devices has decreased, and VR devices become more usable and portable. The price has reached a reasonable range due to easily accessible parts and technology. This technology, which is being applied in more fields thanks to developments in hardware and software technologies, is one of the influential factors that will affect our future.

Virtual reality systems are divided into three categories in the literature as fully immersive, partially immersive, and non-immersive. Systems that surround a participant consist of devices that create a high level of reality feeling such as Head-Mounted Displays (HMD) and Computer Assisted Virtual Environment (CAVE). The partially immersive systems allow more than one user to have simultaneous experiences compared to other systems with high-resolution widescreen screens, creating a feeling of immersion in users. In desktop virtual reality systems, users are involved in virtual activities through only one monitor. However, they cannot feel wholly involved in a virtual environment.

In our study, the virtual environment was presented using the HTC Vive HMD to provide participants with a more realistic and fully immersive experience. Body movements can be detected through the integrated gyroscope of the Htc Vive headset, and thus, users are provided with a more interactive virtual experience. The Htc Vive HMD system consists of two base stations, VR glass, and controllers, as shown in Figure 2.1.. The Htc Vive head mounted display includes two AMOLED displays. Displays are located behind the lens which can be manually controlled on the headset itself to move the lenses in and out. This provides an adjustable interpupillary distance (IPD) (61mm to 72mm) and allows a perfect viewing experience for a wide range of users. The Htc Vive HMD accommodates a total of 2160 x 1200 pixels, 1080 x 1200 pixels per eye. The HTC Vive headset has a refresh rate of 90 Hz and a 110-degree field of view.

FIGURE 2.1. HTC Vive head mounted display

2.2.2 Stereoscopic Vision

The human visual system (HVS) involves an extended range of depth cues. These depth cues are classified into two main categories: visual and physiological cues. Visual cues can be divided into the two subgroups, namely monocular and binocular depth cues, whereas the physiological depth cues, also called oculomotor, include accommodation, vergence, and pupil size control such as constriction or dilation.

2.2.2.1 Oculomotor Depth Cues

The movements of eyes, contraction, and relaxation of eye muscles create a perception of depth, based on the point of view of the pupils to the object. Convergence cues include the movements of the eyes inward while looking at a nearby object. The accommodation cues, on the other hand, when the eye is looking at a distant object, sensing system works by moving eyes away from each other and focusing on the object. When the eyes move inward to focus on the nearby object, the eye muscles tighten to hold the eye lenses. When looking at a distant object, the eye muscles relax because the eyes will move away from each other. The vision system perceives the depth of objects with these movements in the eyes.

2.2.2.2 Visual Depth Cues

In daily life, we always live in a three-dimensional world. This situation requires us to continually evaluate the distance between objects and how much objects occupy the space. We use various cues to determine the depth of space and the distance between objects. Some of these cues are based on a single eye (monocular), and some are based on a double eye (binocular) cues.

- **Monocular Depth Cues:** Some cues on depth can also be provided with a single eye view. Monocular depth cues consist of pictorial and motion-based cues. Pictorial cues include factors of occlusion, cast shadow, shading, linear perspective, relative dimension, texture gradient. Motion-based cues provide us with a perception of depth information during the motion of objects or observers.

- **Binocular Depth Cues:** The eyes are located horizontally on the face, which causes the visual areas of the two eyes to overlap to a certain point. In this way, the resulting stereoscopic vision provides the integration of two retinal images to make the perception of distance and depth more accurate. Human eyes are about 6 cm apart from each other. In this regard, each eye sees the world a little different from each other. This image mismatch between the horizontal positions of our two eyes is called a retinal difference. The amount of difference depends on the relative distance of the objects, giving us a clue about depth. With two eyes open, most of the objects seen stimulate different locations on the two retinas. If the difference between the images in the retinas is small enough, the visual perception system treats them without depth. In other words, the visual perception system produces a perception of the depth of the three-dimensional world by evaluating the horizontal disparity between images.

2.2.3 Stereoscopic Image Generation

In stereoscopic image generation, the most crucial step is the accurate adjustment of the stereoscopic camera parameters. There are two principal parameters for controlling disparity between images in a stereoscopic vision: (camera) interaxial distance and (camera) convergence distance. The disparity is used to perceive the absolute depth information of the observed scene.

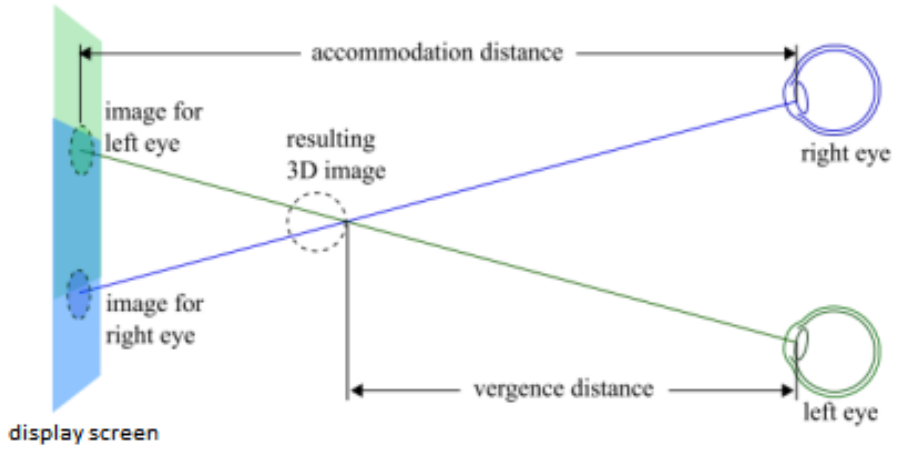

FIGURE 2.2. The vergence–accommodation conflict in stereoscopic displays

In stereoscopic systems, two cameras are placed horizontally in slightly different positions. These cameras are used to represent the left and right eyes. The distance between the cameras is called interaxial separation. The convergence distance corresponds to the distance between the plane where a focused object is located and midpoint between the two cameras. In traditional stereoscopic displays, the scene is physically located on the display screen; however, scene items are displayed around the display screen due to the perception of depth provided. Thus the disparity cue drives the eyes to converge towards scene elements on the perceived depth, while the light coming from the display forced the eyes to focus on the display plane, causing the vergence accommodation conflict as shown in Figure 2.2.. Although people have a degree of tolerance against this conflict, it can contribute to focusing problems, visual fatigue, and eyestrain with long term use, especially if the depth perception is exaggerated.

2.2.4 Cybersickness

Users immersed in a virtual environment (VE) experience motion sickness like discomfort. Symptoms observed in participants exposed to virtual environments, which include nausea, pale skin, cold sweats, vomiting, dizziness, headache, increased salivation, and fatigue, are similar to motion sickness symptoms. However, due to the absence of a real physical movement, this discomfort was evaluated separately from motion sickness and named as cybersickness or visually induced motion sickness in the literature.

Sensory mismatch is widely seen as the leading cause based on the assumption that the external stimulus is perceived differently with different senses. Cybersickness is mainly induced when the perceived movements in a VE are not felt by the vestibular system [11]. Another common reason for the cybersickness experienced in VR environment is the vergence accommodation conflict (VAC). In this complication, the discomfort arises from the conflict between the vergence distance, the distance where the eyes meet on the object of interest, and the accommodation, the distance the eye lenses are adjusted to focus on. In real life, this is not an issue as the vergence distance matches the accommodation. However, in VEs using stereoscopic vision, the objects can be rendered behind or in front of the screen, causing the vergence distance to be on the object while the accommodation is set on the screen. The conflicting information creates a feedback loop which induces discomfort and contributes to cybersickness.

Cybersickness has been widely researched since Kolasinski's work in 1995 [17] where it was mentioned as simulator sickness. Rebenitsch et al. [10]. categorized cybersickness factors as hardware, software, and individual-related factors. In this study, we focus on cybersickness caused by software factors. The review lists many factors possibly contributing to cybersickness and the proposed ways of detection.

Navigation speed, altitude above the terrain, degree of control, vection, screen luminance, contrast, visual background, scene complexity, and stereoscopic rendering parameters in the virtual environment has been investigated in several studies as software cybersickness factors. In this study, we investigated effects of the navigation speed, scene complexity, and stereoscopic rendering parameters on the experienced cybersickness. So et al. [29] found that speed of movement inside a VE had a significant effect on the score of SSQ-O that is related to eye and vision related symptoms. Welch et al. [32] pointed out that increased visual realism in the VE strengthens the sense of presence. However, Jaeger et al. [33] investigated that an increase in the detail level of the scene content caused an increase in SSQ scores. Kolasinski et al. [35] investigated that cybersickness related symptoms become more severe when participant's eyes separation, and the spacing between the virtual cameras differs more.

2.2.5 Electroencephalography (EEG) signals

Human brain is filled with neurons. Every time we feel, think, or intended to move, neurocells are communicating with each other to convey a message. This message is carried out by

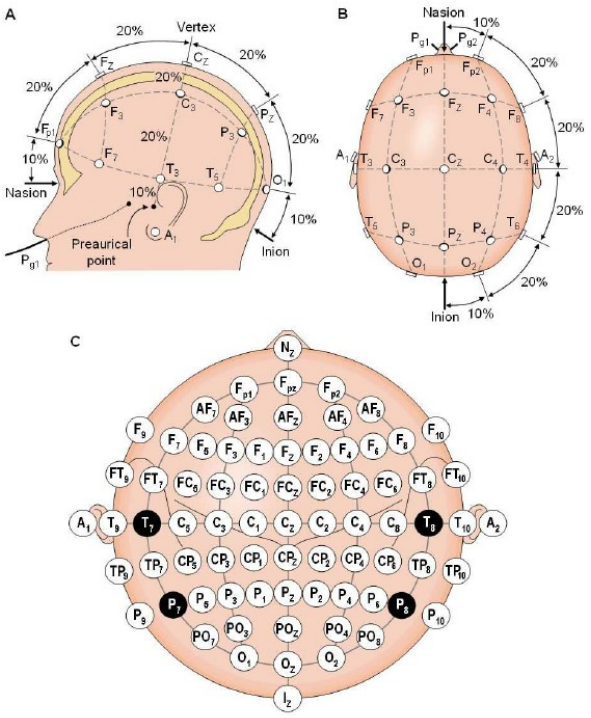

FIGURE 2.3. Different perspectives of the International 10-20 Standard System of electrodes

biochemical and electric signals. Electroencephalography (EEG) is an electrophysiological monitoring method that observes electrical activity of neurons. Although invasive electrodes are sometimes used, as in electrocorticography, mostly electrodes are placed across the scalp and are not invasive. EEG measures the voltage fluctuations from the ionic current inside the brain's neurons. Since EEG signals are collected through electrodes placed on scalp, areas where sensors are placed are of great importance for the analysis of signals and repeatability of experiments, which has led to the need to standardize the positioning of electrodes. EEG electrodes are localized according to the 10-20 system. The 10-20 standard is an internationally accepted method to describe the location of electrodes on the scalp. The numbers in the standard name correspond to the percentage ratio of the distance between adjacent electrodes to the total anterior-posterior or right-left distance of the skull. The location of each electrode in the 10-20 system is identified with a letter and a number that correspond to the lobe and the hemisphere location, respectively, as shown in Figure 2.3.. Even numbers used in identifying localization indicate that the electrode is in the right hemisphere, and odd numbers are in the left hemisphere.

There are three primary sources of information in EEG signals [50]. Spatial information

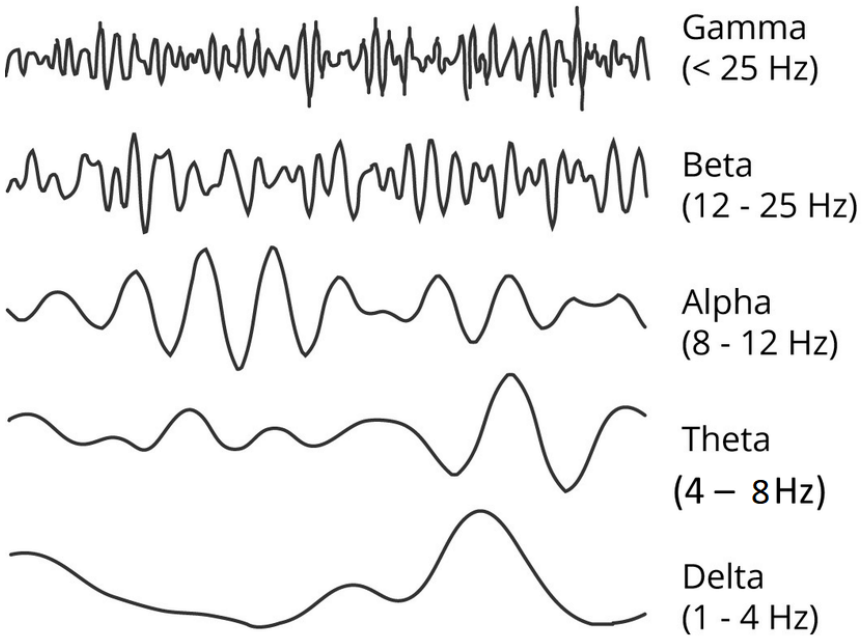

FIGURE 2.4. Frequency Band of EEG Signals

corresponds to the spatial source of the measured signals. Another set of information contained in EEG signals is temporal information. The temporal information describes changes in signals over time. It is mainly used in the The Event-Related Potential (ERP) studies. ERP is the effect of low-frequency response seen after a certain time as a result of a given stimulus. The ERP type activities are easy to detect due to characteristics of the signal and response to a given stimulus within a certain time. Lastly, spectral information means power changes in the selected frequency bands. It is used in BCI studies based on oscillatory activities. Oscillatory activities cause the waves in specific frequency bandwidth to dominate the EEG recordings. EEG signals are generally analyzed based on five frequency bandwidths, as shown in Figure 2.4.. Delta waves occur in deep sleep states, unconsciousness, or when brain activities are deficient. It is prominent in the frontal region in adults and the occipital region in children. Theta waves occur when the brain activities such as deep relaxation, well-being, pensiveness, and emotional tension in adults are still at a level that can be called low. Alpha waves appear in relaxation, meditation, non-arousal, and awake without any concentration state. Beta waves occur in stressful, irritable situations, during repetitive headaches when focus and concentration cannot be achieved. Gamma waves occur in the case of high-level information processing, active learning, concentration, consciousness, and cognitive functioning.

EEG signals have a low signal-to-noise ratio (SNR), and task-related responses may be suppressed by noises and artifacts. Cross-subject variability and poor spatial resolution are the main obstacles in BCI applications. Nunez et al. [51] demonstrated that about half the contribution to a single electrode potential comes from sources within a 3 cm radius of the corresponding electrode. Besides, EEG signals are non-stationary, which may cause the trained model to predict different results even when the model is tested in the user to whom the model is trained.

Chapter 3.

METHODOLOGY

This study consists of two phases, namely the training phase and the feedback phase. Firstly, participants were immersed in a VE consisting of three repeating sessions. In each session, participants go through cues generated with different levels of navigation speed, scene complexity, and stereoscopic rendering parameters. The EEG data collected in the first phase was used as training data for the proposed cybersickness detection and mitigation system (CDMS). The CDMS consists of two consecutive models. In the first model, cybersickness was detected using time-series EEG data. Then, if the result of the first model indicates uncomfortable condition, the factor type that causes cybersickness was classified by performing multi-class classification in the second model. In the second phase of the study, we conducted an experiment using different participants to evaluate the performance of the CDMS. The following sections provide detailed information about the experimental setups, model architectures, participants' information, and the VEs for both the training and the feedback phases. Teaser of this study is shown in Figure 3.1..

3.1. Training Phase Experiment

3.1.1 Participants

A total of 40 participants voluntarily attended the training phase experiment. Due to the hardware and software related faults that occurred during the experiment, data with sufficient

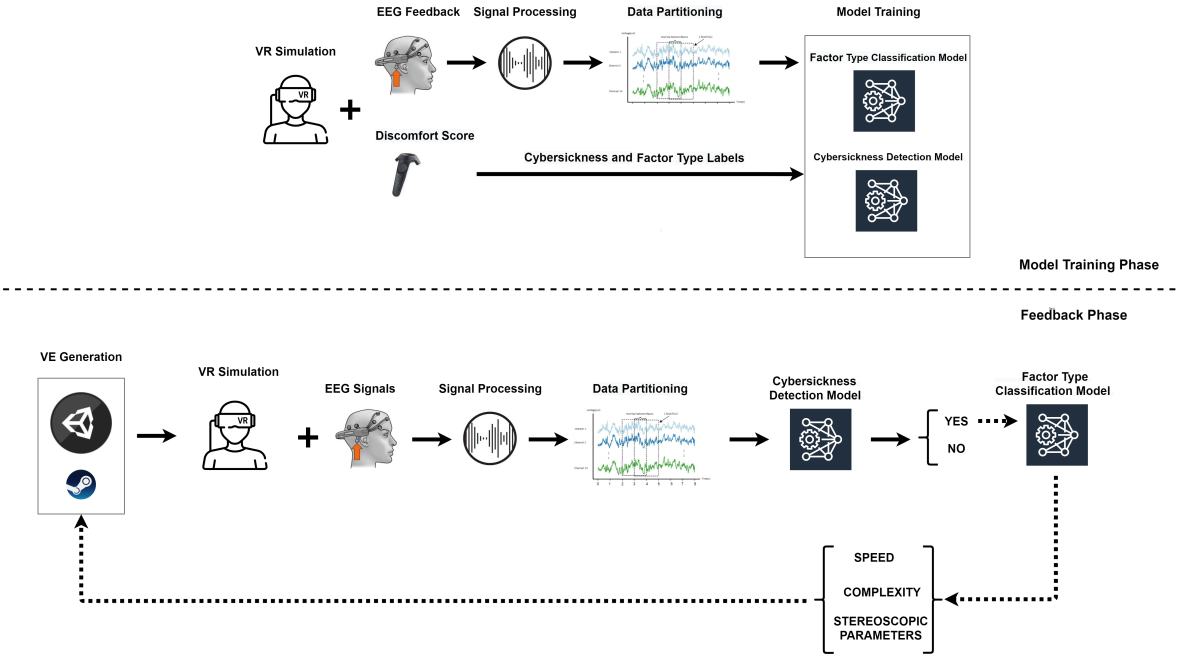

FIGURE 3.1. Plot illustrating the model training (top half) and the feedback (bottom half) phases of the proposed cybersickness detection and mitigation system. In the model training phase, cybersickness factors of navigation speed, scene complexity, and stereoscopic rendering parameters were simulated separately in the virtual environment (VE). EEG data and general discomfort scores were collected during the sessions to train a two-stage shallow CNN model to detect cybersickness and to classify factor type. In the feedback phase, the trained models are used in the loop to detect and mitigate cybersickness in real-time by updating the VE generator simultaneously to adjust the identified factor.

qualification could not be collected from 5 out of 40 participants. Besides, the data collected from two participants were not included in the training data as they reported that they did not feel cybersickness in any of the cues. Our final sample consisted of 33 people aged between 18 and 42 (mean = 23.8). Seven participants were female, and 26 of them were male. The participants had an average MSSQ percentile of 29.7. Overall they had little experience with VR (0.9 average on a 0-4 scale(0: Not at all familiar, 4: Extremely familiar)) and moderate game habits (2.1 average on a 0-4 scale(0: Never, 4: Always)).

3.1.2 Procedure for the Model Training Phase

The training phase experiment was conducted in three repeating sessions. Each session started with a baseline cue that is stationary and does not have any external stimulus. The baseline cue is applied to receive EEG data in the steady-state of brain waves. After the

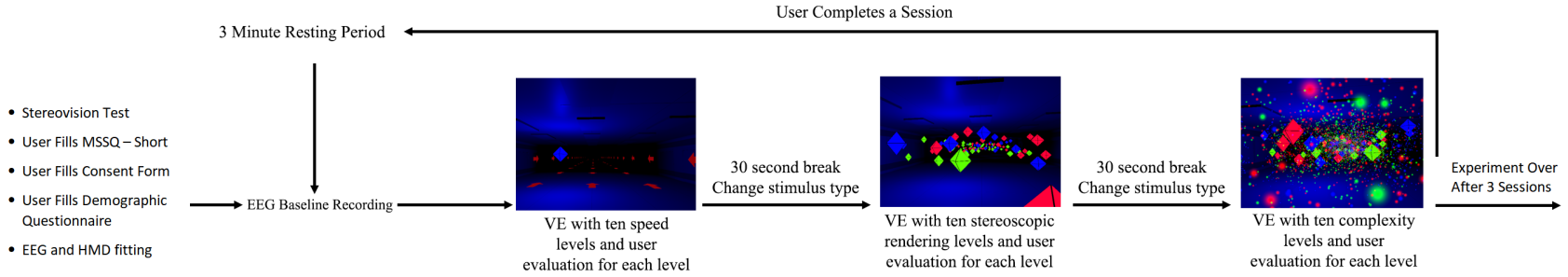

FIGURE 3.2. Flowchart of the experimental procedure for the training phase

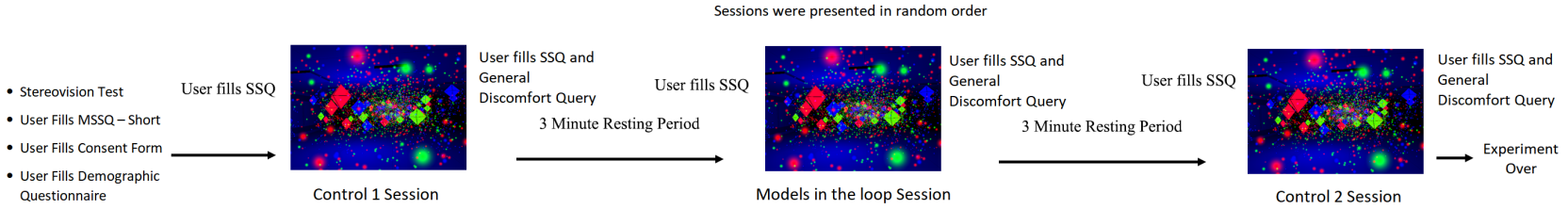

FIGURE 3.3. Flowchart of the experimental procedure for the feedback phase

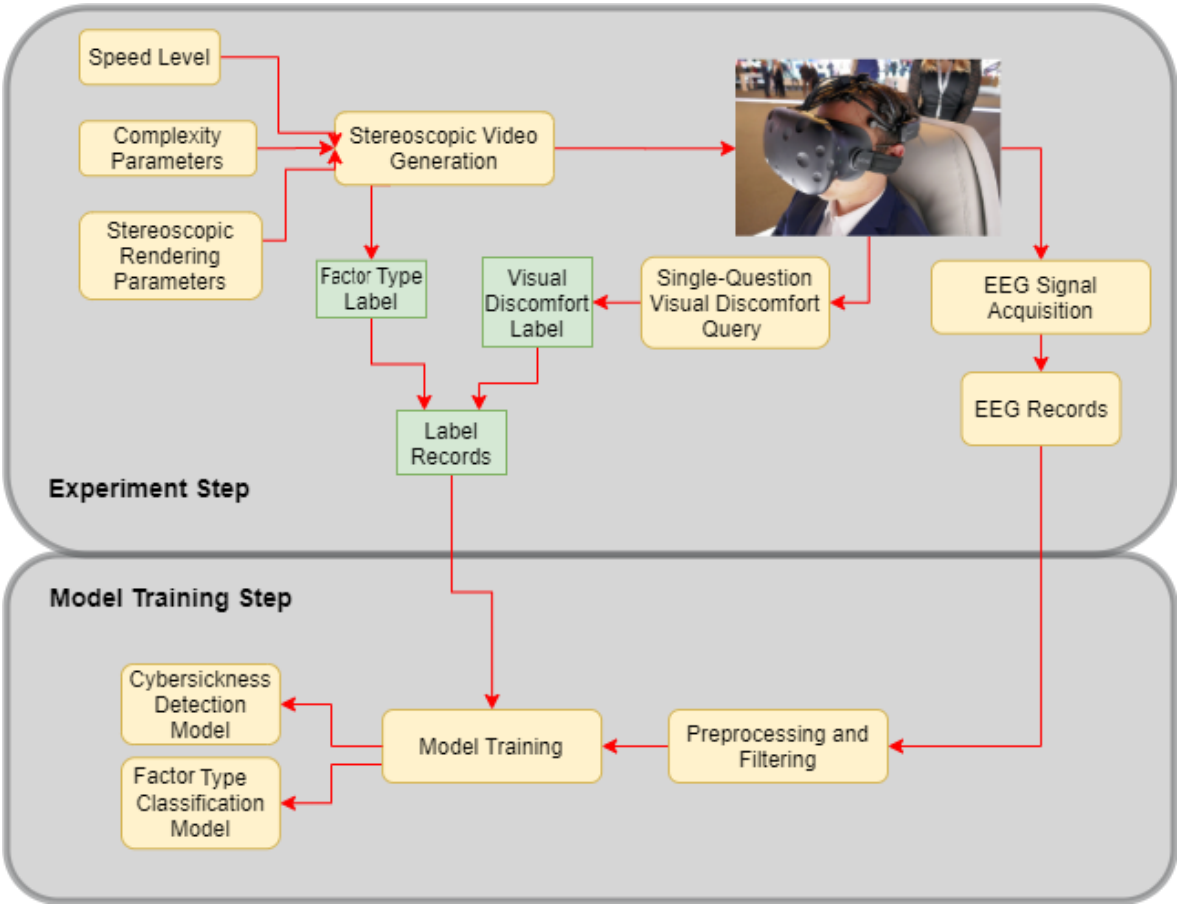

FIGURE 3.4. Flowchart of the experiment and model training steps for the training phase

baseline cue, participants were immersed in a VE consisting of three types of cues in each session. Cues that were created using ten levels of navigation speed, seven levels of scene complexity, and ten different stereoscopic rendering parameters sets presented to the participants in a random order, with 30 seconds rest period between them to avoid cybersickness accumulation. The baseline and each cue level takes ten seconds. At the end of each cue, users were asked to rate the severity of experienced cybersickness on a scale ranging from 1(”none”) to 7(”extreme”). The participants were given a 3-minute rest period before proceeding to the next session. Flowchart of the experiment and model training steps for the training phase is shown in Figure 3.4..

Experiments were carried out in a silent and external stimulus-free environment where a participant sits on a fixed seat. In this way, probable noise and artifacts were reduced, and a safer test environment was offered to the participants during the experiment. The overview of

the experimental procedure of the training phase is given in Figure 3.2.. The training phase experiment was comprised the following steps:

- Participants were subjected to a stereo-blindness test where they were shown a random-dot stereogram to confirm that they do not have any stereoscopic vision disability before the experiment. It was also confirmed that participants had not experienced epilepsy seizures before to avoid the risks that may occur during the experiment. Each participant was informed about the experiment, and they were asked to fill out the consent form.
- In order to identify possible outlier data more efficiently, participants' game habits, VR experiences, and demographic information were asked, and the MSSQ (Motion Sickness Susceptibility Questionnaire) was applied to measure their susceptibility to motion sickness.
- The HMD equipment and EEG electrodes were fitted onto the participant's head. The Emotiv Cortex API was utilized to ensure the reliable signal quality for each channel.
- Each training session started with a baseline cue. Then, participants were immersed in factor sets containing different levels, with a 30-second rest period between each. Participants were asked to rate the severity of experienced cybersickness on a scale ranging from 1("none") to 7("extreme") at the end of each level.
- When a session ended, participants were given a no less than 3-minute rest period before proceeding to the next session. The rest period was extended for the participants who did not feel well after this period.
- EEG data and labels, including factor types and the general discomfort scores participants rated after corresponding cue in the training phase experiment, were recorded for use in the model training.

The software infrastructure used in the model training experiment was designed, as shown in Figure 3.5.. The virtual environment created by using the Unity Game Engine is presented to users via the HTC Vive VR headset by using SteamVR. The raw EEG data collected simultaneously from users are recorded in the Emotiv cloud storage by the Emotiv Cortex API. The username, session name, markers indicating factor type, start and stop recording commands required for saving EEG data are sent from Unity game engine to the Emotiv

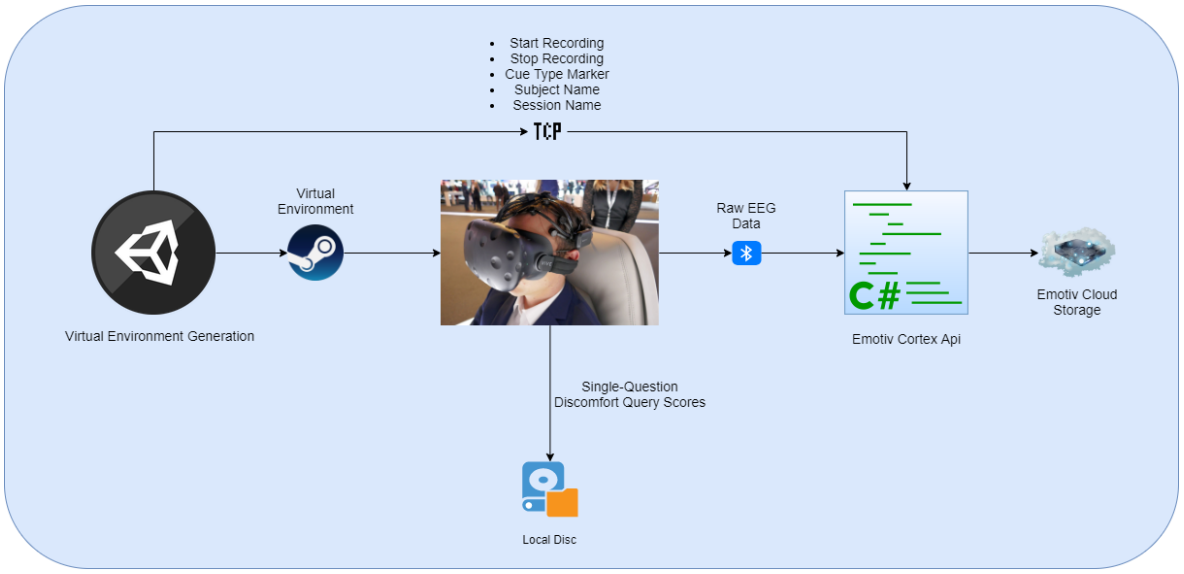

FIGURE 3.5. The software infrastructure for the training phase

Cortex API over TCP-IP. Besides, general discomfort evaluation scores collected from users after each cue are stored on the local disk.

3.1.3 Virtual Environment for the Training Phase

The virtual environment used in the study was created using the Unity Game Engine and the SteamVR. The participants were immersed in the VE with an HTC Vive HMD headset, which runs at 1080x1200px resolution per eye and 90 Hz refresh rate. In both phases of the experiments, the participants moved along a dark corridor environment generated with different navigation speed, scene complexity, and stereoscopic rendering parameters. Participants were asked to follow a focus object, a blue glowing octahedron, with their eyes and/or their head. The object to be tracked oscillated to the left and right while moving equivalent to the navigation speed of a participant. Sample frames for each factor type were given in Figure 3.2..

The most crucial step in creating a stereoscopic image is the correct adjustment of the stereoscopic camera parameters. Convergence distance is the parameter used to define the distance between the camera plane and the focus plane. Another stereoscopic parameter is the interaxial distance, which is defined as the distance between the cameras. The perceived depth can be modified in the stereoscopic vision by adjusting these parameters. In the training

phase experiment, only one of the stereoscopic rendering parameters was changed between consecutive levels. The stereoscopic cue started with a moderate inter-axial distance and a short convergence distance. An increase in the convergence distance was followed by an increase in the inter-axial distance after the convergence distance reaching its maximum value. After the inter-axial distance reached its maximum value, the convergence distance value was decreased between consecutive levels. The smaller clones identical with the focused object were scattered with randomized colors in the background to increase the number of depth cues. They were kept smaller as not to take focus away from the main object. Each of the stereoscopic rendering levels takes ten seconds.

To investigate the effect of navigation speed, a parameter set was constructed with 10 different navigation speed levels, which starts from 1.2 meters/sec, increases between consecutive levels, and reaches 76meters/sec at the highest level. The increase in navigation speed starts exponentially in the first half, and the latter half proceeds linearly. Since the participants were less disturbed at low and very high speeds, fewer samples were taken at low speeds, and more samples were taken at medium and higher speeds. In order not to induce a complexity-related cybersickness and to invoke the sense of vection, only the object to be followed and bright red arrows on the surrounding walls and floor were included in the VE. An emission shader is applied to the red arrows that allows them to be seen independently from the focus object position as it is the only light source in the environment. Each of the navigation speed levels takes ten seconds.

We also evaluated the impact of scene content on cybersickness by generating cues with seven levels of complexity. At the first level, there was only the object to be followed in the presented scene. At the second level, clones identical to the followed object were positioned towards the outside of the corridor environment and oscillating vertically in a sinusoidal pattern. At the following level, the copies of the focused object were distributed randomly throughout the VE, with more than the second level. At the fourth level, the scene contents were identical to those in the third level, but they were randomly colored as red, green, or blue. Particle emitters attached to the clones at the fifth level. At the sixth level, the particles are given HDR texture to make them brighter, and a particle force field was used to propel the particles further into the participant's view. At the final level, the amount and brightness of emitted particles were maximized to induce more cybersickness. The scene contents of other factors were kept as minimal as possible in order to isolate the effects of manipulating scene complexity cue to this factor scene only. Each of the complexity levels takes ten seconds.

3.2. Feedback Phase Experiment

3.2.1 Participants

In the feedback phase, 22 participants voluntarily took part in the experiment. One participant wanted to withdraw from the experiment after the Control 1 session because he experienced severe cybersickness. On the other hand, one participant was not included in the experiment because he failed in the stereo blindness test. All procedures applied to participants before the training phase experiment were applied at this stage as well. Contrary to the training phase, participants asked to fill out the SSQ at the beginning and at the end of each session in addition to the single-question general discomfort query. The age of the participants varied between 22 and 33, with an average of 28.1. All participants were male. The average MSSQ percentile of the participants was 29.05. They had little experience with VR (0.85 average on a 0-4 scale(0: Not at all familiar, 4: Extremely familiar)) and moderate game habits (1.1 average on a 0-4 scale(0: Never, 4: Always)).

3.2.2 Procedure for the Feedback Phase

In the feedback phase, we aim to classify the type of cue causing cybersickness with the models trained in the model training phase and to mitigate cybersickness by updating the relevant cue parameters to provide a more comfortable vision. The feedback phase experiment consists of three consecutive sessions. In control 1 and control 2 sessions, participants were immersed in a VE in which the cue parameters were updated following specific templates as shown in Figure 4.9.. However, in models in the loop session(MIL), the cue parameters were updated simultaneously following the feedback from the cybersickness detection and factor type classification models. The sessions were presented to the participants in a random order and the participants did not know in which session the cybersickness mitigation model was activated. Participants asked to fill out the SSQ at the beginning and the end of each session to evaluate the performance of the cybersickness detection and mitigation system (CDMS). Moreover, participants were requested to rate the severity of experienced cybersickness with the single-question discomfort query on a scale ranging from 1(”none”) to 7(”extreme”) at the end of each session. The overview of the experimental procedure of the feedback phase is given in Figure 3.3..

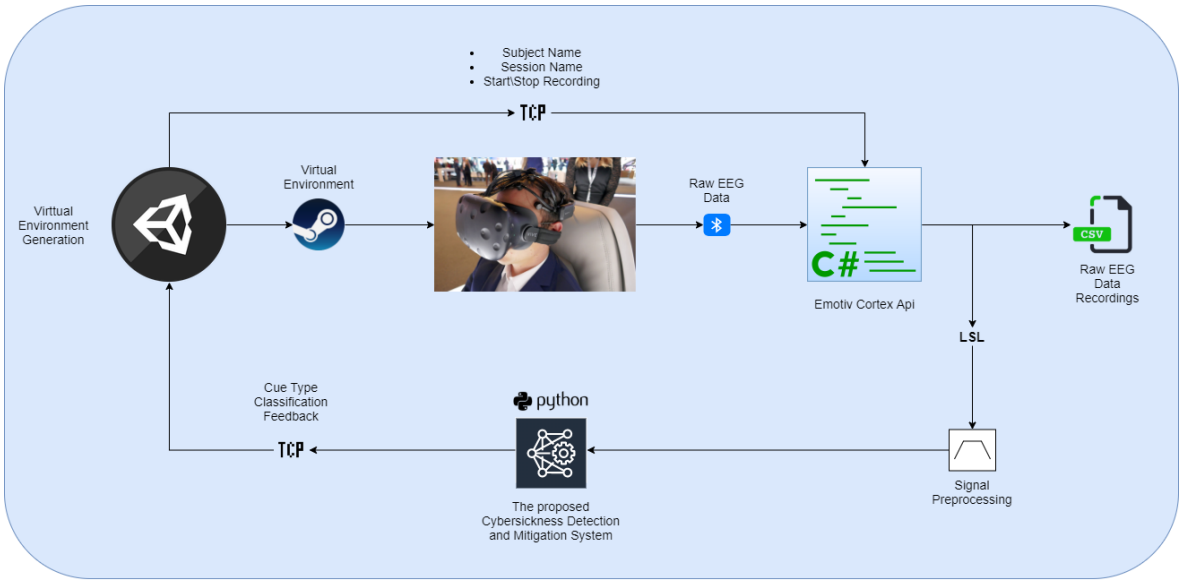

FIGURE 3.6. The software infrastructure for the feedback phase

The feedback phase experiment was comprised the following steps:

- Participants were subjected to similar procedures in the training phase experiment, and the experiment is initiated after the participant has been confirmed to be suitable for the experiment.
- Participants filled the MSSQ, game habits, VR experiences, and demographic questionnaires.
- The HMD equipment and EEG electrodes were fitted onto the participant's head. The Emotiv Cortex API was utilized to ensure the reliable signal quality for each channel.
- Participants asked to fill out the SSQ at the beginning and the end of each session.
- Participants were immersed in two control and MIL sessions, which were presented in random order with a minimum of 3 minutes of rest period between them.
- After each session, participants were requested to rate the severity of experienced cybersickness with the single-question discomfort query on a scale ranging from 1(”none”) to 7(”extreme”).

The software infrastructure used in the online experiment was designed, as shown in Figure 3.6.. The virtual environment created using the Unity Game Engine is presented to users

with the HTC Vive VR headset using SteamVR. The raw EEG data collected from the users are simultaneously transferred to the cybersickness detection and classification models developed in the Python environment by using the Lab Streaming Layer communication protocol by the Emotiv Cortex API. At the same time, all EEG data is stored on a local disk in CSV format to create a comprehensive EEG database. The username, session name, start, and stop recording commands required to save EEG data are sent from the Unity game engine to the Emotiv Cortex API over TCP-IP. Finally, the factor type feedback that causes cybersickness classified by the proposed model is transmitted to the Unity game engine to perform the necessary parameter updates over TCP-IP.

3.2.3 Virtual Environment for the Feedback Phase

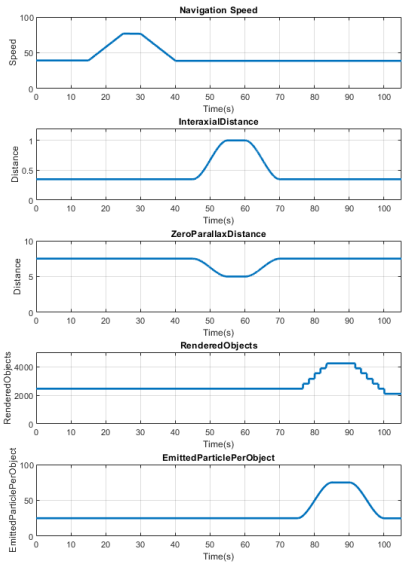

FIGURE 3.7. Time-dependent changes in the cue parameters of the control 1 session

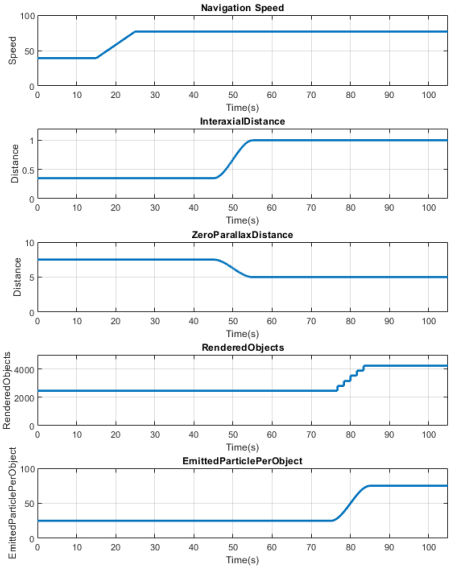

FIGURE 3.8. Time-dependent changes in the cue parameters of the control 2 session

In the feedback phase, we conducted an online experiment that consists of two different control sessions and one models-in-the-loop (MIL) session. The number of rendered objects and the number of particles released from each object parameters were used to control scene complexity. Similarly, inter-axial distance and convergence distance parameters were utilized

as stereoscopic rendering parameters to induce different levels of cybersickness. Sample frames for each factor type were given in Figure 3.3..

In the control 1 session, the virtual scene started with a moderate level of speed, complexity, and stereoscopic rendering parameters. Afterward, speed, complexity, and stereoscopic rendering parameters were shifted according to a specific template as shown in Figure 3.7.. Before the parameters of each factor were shifted, the previously shifted parameters were reverted to the initial state, and then five seconds would pass. Cue parameters were fitted to specific functions to make the transition smooth and hence not to lose the feeling of presence.

In the control 2 session, the virtual scene was created similar to the control 1 session. The only difference was that the shifted parameters remain at a level that induces the maximum level of cybersickness until the end of the session. The time-dependent changes in the speed, complexity parameters, and stereoscopic rendering parameters for control 2 session are shown in Figure 3.8.. The MIL session was created based on the template of control 2 session. From the moment the MIL session started, the corresponding cue parameters were updated by a fixed step following the feedback from the classification model. However, each parameter was shifted by a fixed amount starting from the last level of the corresponding parameter at the time step that it needs to be shifted in accordance with the template of the control 2 session.

3.3. Data Acquisition

We use the Emotiv Epoc+ EEG measurement headset in this study. The Emotiv Epoc+ headset has been widely used equipment in BCI experiments since it meets the needs for low cost and high mobility. The Emotiv Epoc+ headset has 14 saline-based electrodes plus two reference electrodes, an inertial gyroscope, and an accelerometer to measure head movement during the experiment. Thanks to wireless connection, it is suitable for studies requiring high mobility [1]. All the features of the Emotiv Epoc+ headset are shown in Table 3.1..

EEG electrodes are positioned according to the 10-20 system, as shown in Figure 3.9.. The 10-20 standard is an internationally recognized method to describe the location of electrodes on a scalp. This system was accepted as a standard to maintain standardized testing methods

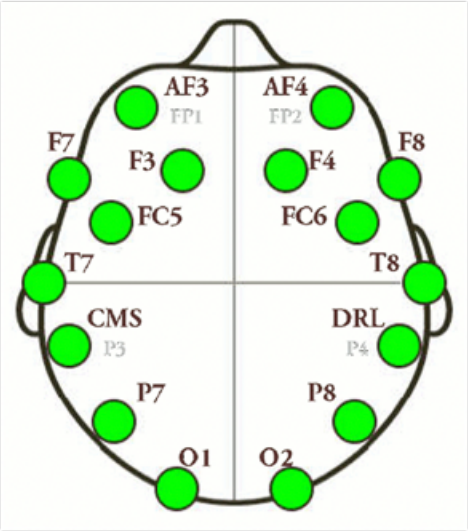

FIGURE 3.9. Electrode locations of the Emotiv EPOC+ headset. The upper part shows the front of the head. Adapted from [1]

that allow collected data to be compiled, effectively analyzed, and compared with data collected from different subjects using the scientific method. We utilize the Emotiv Cortex API to evaluate the signal quality for each channel. The signal quality rank on scale of 1 (”no signal”) to 4 (”good”) indicates the accuracy of receiving data for each channel.

EEG data are collected at 2048 Hz internally. However, it is transmitted as 128 or 256 Hz according to the user's preference. In our study, EEG signal was collected with a sampling rate of 256 Hz. A bandpass filter is applied to the raw EEG data to collect data covering the frequency bands of theta (4 to 8Hz), alpha (8 to 12Hz), beta (12 to 25Hz), and gamma (25 or more). Delta (0.2 to 4Hz) frequency band is excluded in this study because delta waves occur in deep sleep states, unconsciousness, or when brain activities are deficient. We do not need to apply the notch filters, because 50Hz-60Hz notch filters are implemented in the hardware internally.

During the training phase, raw time-series EEG data and markers indicating factor type within each session were recorded simultaneously using the Emotiv Cortex API with the edf extension. Three edf files, one for each session, were obtained per participant. We used the EEGLAB toolbox [52] in Matlab computational software for data preprocessing and partitioning the data recorded in batches per session by factor type. The partitioned EEG data were labeled according to the participants' general discomfort score and the corresponding factor type.

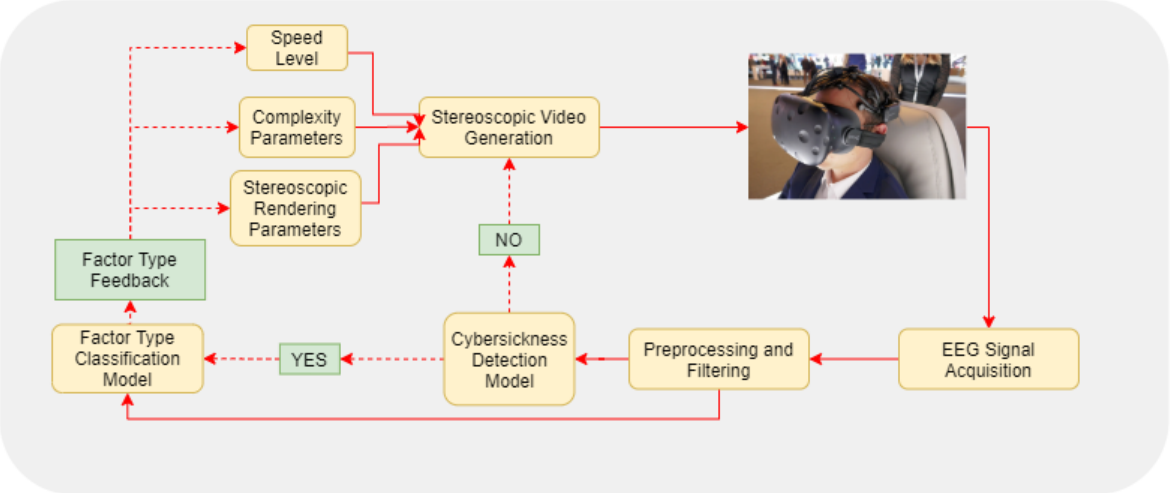

FIGURE 3.10. Flowcart for the Cybersickness Detection and Mitigation System(CDMS)

In the feedback phase, EEG signals are fed to the cybersickness detection model first after being preprocessed using the Lab Streaming Layer interface via Emotiv Cortex API, which was triggered as soon as the scene starts in the VE. If cybersickness is not detected, there will be no update in the cue parameters, and the same scene continues to be presented. If the cybersickness detection model detects cybersickness, the same preprocessed data are fed to the second model as well. Relevant cue parameters are updated in line with the model's feedback, which indicates the type of cue causing cybersickness. The main flow diagram of the CDMS is shown in Figure 3.10.. EEG data collected during both control sessions and the MIL session were logged with the csv extension to create a comprehensive cybersickness EEG database.

3.4. Cybersickness Detection and Factor Type Classification Using Deep Learning Approaches

EEG is a method that monitors the electrical activity occurs as a result of interaction between neurons in a brain. EEG waves differ in amplitude, frequency, and shape according to the brain's (physiological or psychological) state. Cross-subject variability and poor spatial resolution due to volume conduction are the main obstacles in EEG applications. Besides, EEG signals have a low signal-to-noise ratio (SNR), and task-related responses may be suppressed

TABLE 3.1. Specification of the Emotiv EPOC+ headset

Number of Channels	14 (plus CMS/DRL references, P3/P4 locations)
Channel names (International 10-20 locations)	AF3, F7, F3, FC5, T7, P7, O1, O2, P8, T8, FC6, F4, F8, AF4
Sampling Method	Sequential sampling. Single ADC
Sampling Rate	128 SPS / 256 SPS (2048 Hz internal)
EEG Resolution	14 bits 1 LSB = 0.51uV (16 bit ADC, 2 bits instrumental noise floor is discarded), settings can be changed to 16-bit
Bandwidth	0.2 - 45Hz, digital notch filters at 50Hz and 60Hz
Filtering	Built-in digital 5th order Sinc filter
Connectivity	Proprietary 2.4GHz wireless, BLE and USB (Extender only)
Impedance Measurement	Real-time contact quality using patented system
Gyroscope	3-axis +/- 500 dps
Motion Sampling	32 / 64 / 128 Hz (User Defined)
Sensor Material	Ag/AgCl + Felt + Saline

by noises and muscle activity-related artifacts. Therefore, to reveal the task-related information in EEG studies, it is necessary to remove noise and artifacts caused by eye and muscle movements. However, these preprocessing steps are not feasible for use in studies conducted online in terms of computation costs. Artificial neural network approaches provide higher generalization skills and adaptive applications. The popularity of neural network approaches has been increasing in recent years thanks to its ability to handle complex data. This makes it possible not to perform preprocessing, artifact removing, and feature extraction processes, which require high computation power and expertise in the EEG signal processing.

The first step of developing a brain-computer interface application using EEG signals is to know what kind of effect the activity desired to detect has on the brain. These effects are commonly divided into two categories. The Event-Related Potential (ERP) is the effect of high amplitude and low-frequency response seen after a certain time as a result of a given stimulus. The ERP type activities are easy to detect due to characteristics of the signal and response to a given stimulus within a certain time. However, oscillatory activities are not easy to detect because they are associated with power changes in the specific frequency

band, asynchronous, and have a poor spatial resolution due to volume conduction. Cybersickness is not a momentary response but a cumulative effect that occurs after a certain time of exposure. Therefore, we used the Shallow Convolutional Network based on the FBCSP algorithm to detect cybersickness, which is considered as oscillatory activity. The Shallow ConvNet architecture based on the FBCSP was proposed by Schirrmeister et al. [5] and showed outstanding performance on oscillatory signal classification.

At the beginning of our study, we aimed to rate the cybersickness using regression approaches in line with general discomfort assessments scores collected from users. However, since the number of participants is limited and the distribution of the general discomfort scores collected from the users for different levels of each factor strengthens the cybersickness rating by regression, we decided to do the disturbance detection with a classification approach. The proposed cybersickness detection and mitigation system consists of two consecutive models. In the first model, cybersickness experienced in a VE is classified as binary. The first model was trained according to whether the users feel visual discomfort or not, by using all recorded EEG data. The second model was trained to classify factor type that caused cybersickness by using the data that corresponds to cybersickness condition. We first wanted to classify the proposed two-stage cybersikness detection and factor type classification models using a combined multiple classification approach. However, the classification accuracies we obtained revealed that the combined approach performed worse than the separate model approach.

3.4.1 Spatial Filtering

The brain-computer interface (BCI) aims to classify the mental states of users using the collected EEG data. There are three primary sources of information in BCI studies [50]. Spatial information corresponds to the spatial source of the measured signals. To utilize this information, it is necessary to know which parts of a brain are sensitive to the task to be decoded. The visual information is first processed in the occipital lobe, and then depending on its purpose, visual information follows a ventral or dorsal stream, as shown in Figure 3.11. [53] [2]. The P7, P8, O1, and O2 channels of the Emotive Epoc+ headset are located on the corresponding scalp area. However, due to the volume conduction between electrodes and using deep learning in the classification of cybersickness in this study, we decided to use raw EEG signals from all electrodes.

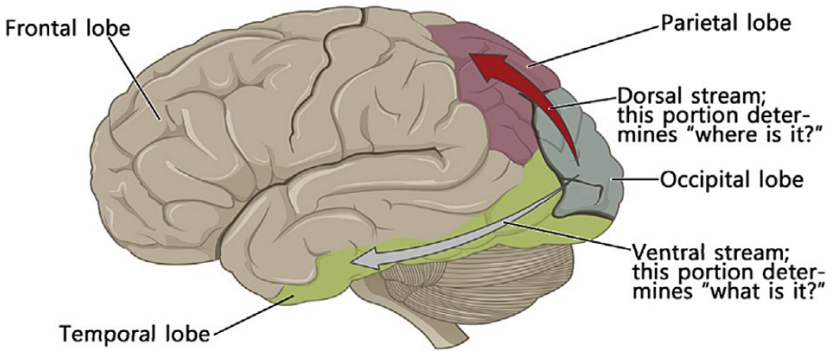

FIGURE 3.11. Two-streams hypothesis of the neural processing of human vision. Adapted from [2]

Another set of information used in brain-computer interface studies is temporal information. The temporal information describes changes in signals over time. It is mainly used in studies where a time-dependent response is expected a certain time after a given stimulus. Lastly, spectral information means power changes in the selected frequency bands. It is used in BCI studies based on oscillatory activities. In most of the studies in the literature, cybersickness is correlated with band power. Information about these studies was detailed in the literature review section. An increase in the EEG signal power in a given frequency band is called the Event-Related Synchronisation (ERS), whereas a decrease in the EEG signal power is called an Event-Related Desynchronisation (ERD). In oscillatory based BCI studies, changes in specific frequency bands are monitored by the specified region of a brain. Therefore, spatial information is needed to be utilized in spectral-domain studies.

The EEG signals have a poor spatial resolution due to volume conduction. Nunez et al. demonstrated that about half the contribution to a single electrode potential comes from sources within a 3 cm radius of the corresponding electrode [51]. The Common Spatial Patterns (CSP), which was designed by Ramoser et al., is frequently used in BCI studies because it enhances the task-related information in the EEG signal while suppressing undesirable activities [54]. The CSP can be implemented easily and is computationally efficient. The performance of the CSP algorithm depends on the operational frequency band. Therefore it provides low accuracy when EEG data is unfiltered, filtered inadequately, or filtered in an inappropriate frequency band. Also, the CSP algorithm tends to overfit if there is not enough training data. To address these problems, Ang et al. proposed a machine learning approach called the Filter Bank Common Spatial Pattern (FBCSP) for processing EEG measurements in motor imagery-based BCI [3]. The FBCSP algorithm is widely used in the EEG signal

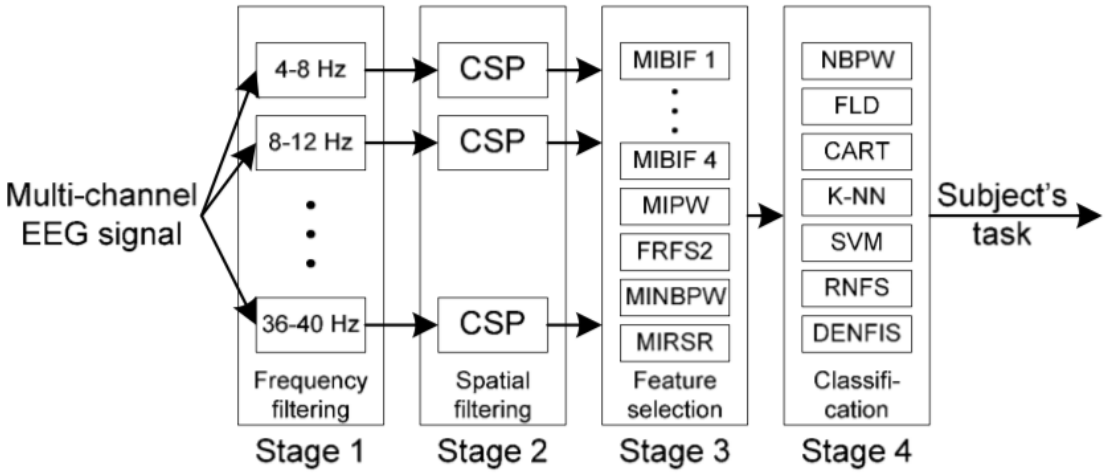

FIGURE 3.12. Architecture of the FBCSP algorithm. Adapted from [3]

classification and has won many EEG classification competitions such as BCI Competition IV 2a and 2b [55].

3.4.1.1 Filter Bank Common Spatial Pattern

The main flow of the FBCSP approach is illustrated in Figure 3.12.. Technically, the FBCSP algorithm computes linear combinations of EEG channels to extract particular band power features. In the FBCSP approach, before applying the CSP algorithm, the EEG signals are separated into multiple frequency bands using bandpass filters. The CSP algorithm is then applied separately for each band. A feature extraction algorithm is employed to extract discriminating features for each frequency band. Finally, a proper classification algorithm is performed for classification by using the extracted features.

3.4.2 Architecture of the Shallow Convolutional Neural Network

Schirrmeister et al. [5] designed the Shallow ConvNet architecture inspired by the FBCSP algorithm to classify oscillatory activities. The architecture of the shallow convolutional network consists of two convolutional layers: one for temporal and one for spatial convolution to deal with variations in spatial and spectral domains. The bandpass and the CSP filtering steps of the FBCSP algorithm are performed as a temporal and spatial convolution in this architecture. Convolutions were utilized to generate an EEG-specific model that extracts

discriminative EEG features. After two convolutional layers, batch normalization is used to standardize values in the hidden layers of the network. A squaring activation function, a mean pooling, and a logarithmic activation function are applied following batch normalization step to extract log band power features. The dropout technique is used to prevent an over-fitting problem. Lastly, a dense softmax layer is utilized for classification.

We trained both models with the Adam optimization algorithm, which is designed to work well with high-dimensional parameters with a learning rate of $6x10^{-4}$ [56]. The training was carried out by minimizing the categorical cross-entropy loss function. We ran 1000 epochs with setting the batch size to 64 and save the model weights, which produced the highest validation accuracy. Architectures of the shallow convolutional networks are shown in Figure 3.13. and Figure 3.14. respectively for the cybersickness detection and the factor type classification models. In the first model in which cybersickness was detected, we set the number of filters used in the first and second convolution layers to 40 with kernel size of 1x25 and 14x1 respectively. On the other hand, in the model in which the factor type was classified, we set the number of filters used in the first and second convolution layers to 50 with kernel size of 1x25 and 14x1 respectively. All models were trained in Tensorflow [57], using the Keras API [58].

We also compare the performance of the Shallow Convolutional Neural Network to that of the Deep ConvNet and EEGNet approaches. The EEGNet architecture consists of a temporal convolution and a depth-wise convolution to perform the bandpass and the CSP filtering steps of the FBCSP algorithm, respectively. A separable convolution and a point-wise convolution are applied following depth-wise convolution to extract temporal features. The architecture of the EEGNet algorithm is visualized in Figure 3.15.. In this way, the EEGNet approach effectively generalizes to both ERP and oscillatory type EEG classification [4].

The Deep ConvNet architecture is developed by Schirrmeister et al. [5] to be a general purpose approaches for both ERP and oscillatory based task classification. The architectureof the Deep ConvNet consists of five convolutional layers and a softmax classification layer. Similar to the EEGNet approach, the bandpass and spatial filters steps are simulated in the first two convolution layers. The architecture of the Deep ConvNet algorithm is demonstrated in Figure 3.16.. Since both approaches are designed for general purpose to cover both the ERP and oscillatory type EEG decomposition, temporal information is extracted from the EEG signal in addition to extracting features related to log band-power.

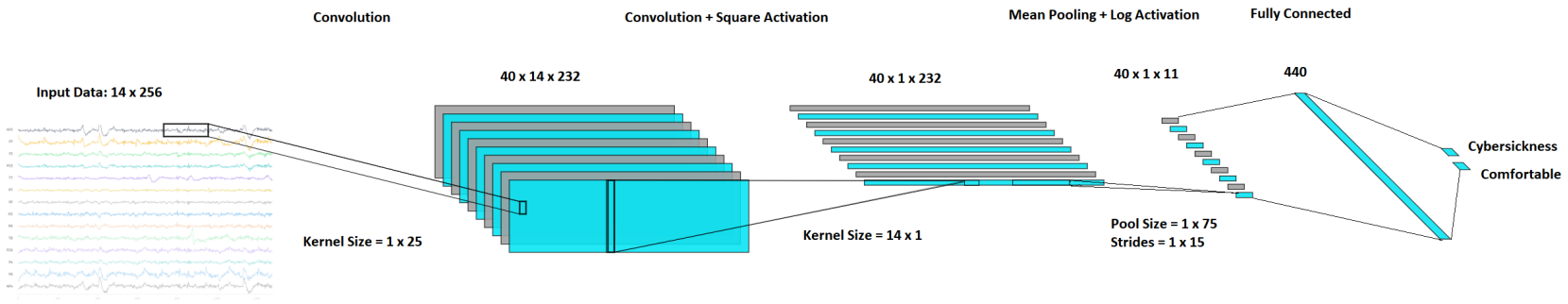

FIGURE 3.13. Architecture of the cybersickness detection model

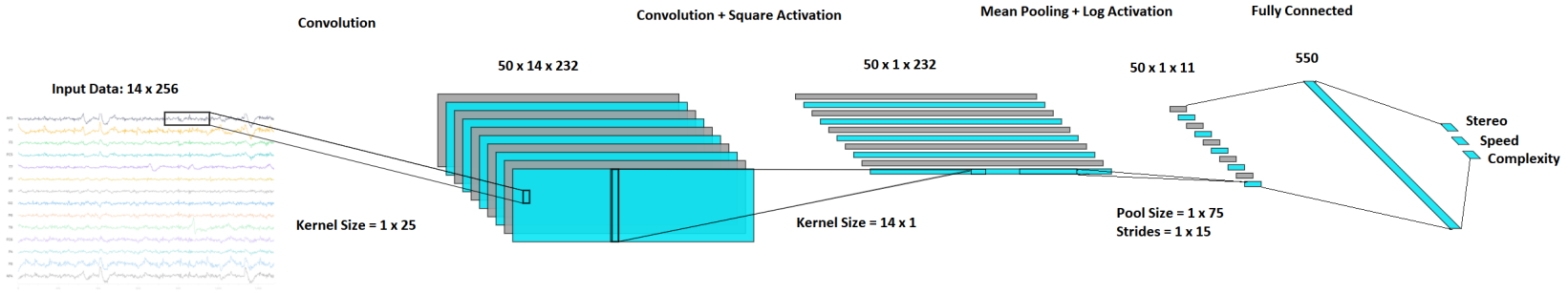

FIGURE 3.14. Architecture of the factor type classification model

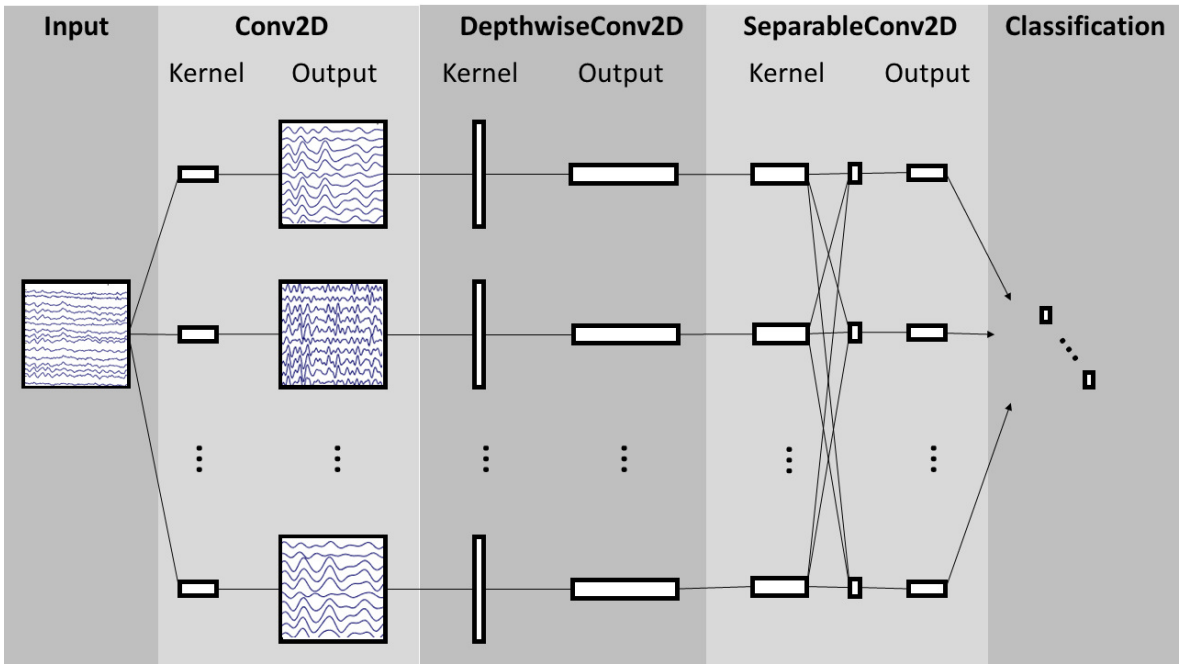

FIGURE 3.15. The architecture of EEGNet algorithm. Adapted from [4]

3.4.3 Data Preparation for the Proposed Models

The raw time-series EEG data from 33 participants were recorded simultaneously in the three repeating sessions of the training phase experiment, including baseline cues at the beginning of each session. EEG data of ten seconds were collected from the participants for each level of cues. At the end of each cue, participants were asked to evaluate the experienced cybersickness severity by using a single-question discomfort query. Label values to be used in the cybersickness detection model were determined by assuming that the discomfort rating scores of two and above indicate cybersickness condition. Data tagged as cybersickness in the first model were also labeled as speed, complexity, and stereoscopic, depending on the corresponding type of cue presented during the recording process.

In order to use multi-channel time-series raw EEG signals as input in the artificial neural network-based classification algorithm, EEG data were subjected to certain preprocessing. Initially, bandpass filtering was applied with a causal third-order Butterworth filter. Then, ten seconds of data recorded during each cue were cut to eight seconds by trimming one-second portions from the beginning and the end. In this way, possible synchronization problems and delays were eliminated. Then, eight seconds of data were divided into pieces in one second using the sliding window, as shown in Figure 3.17.. The partitioned one-second data were

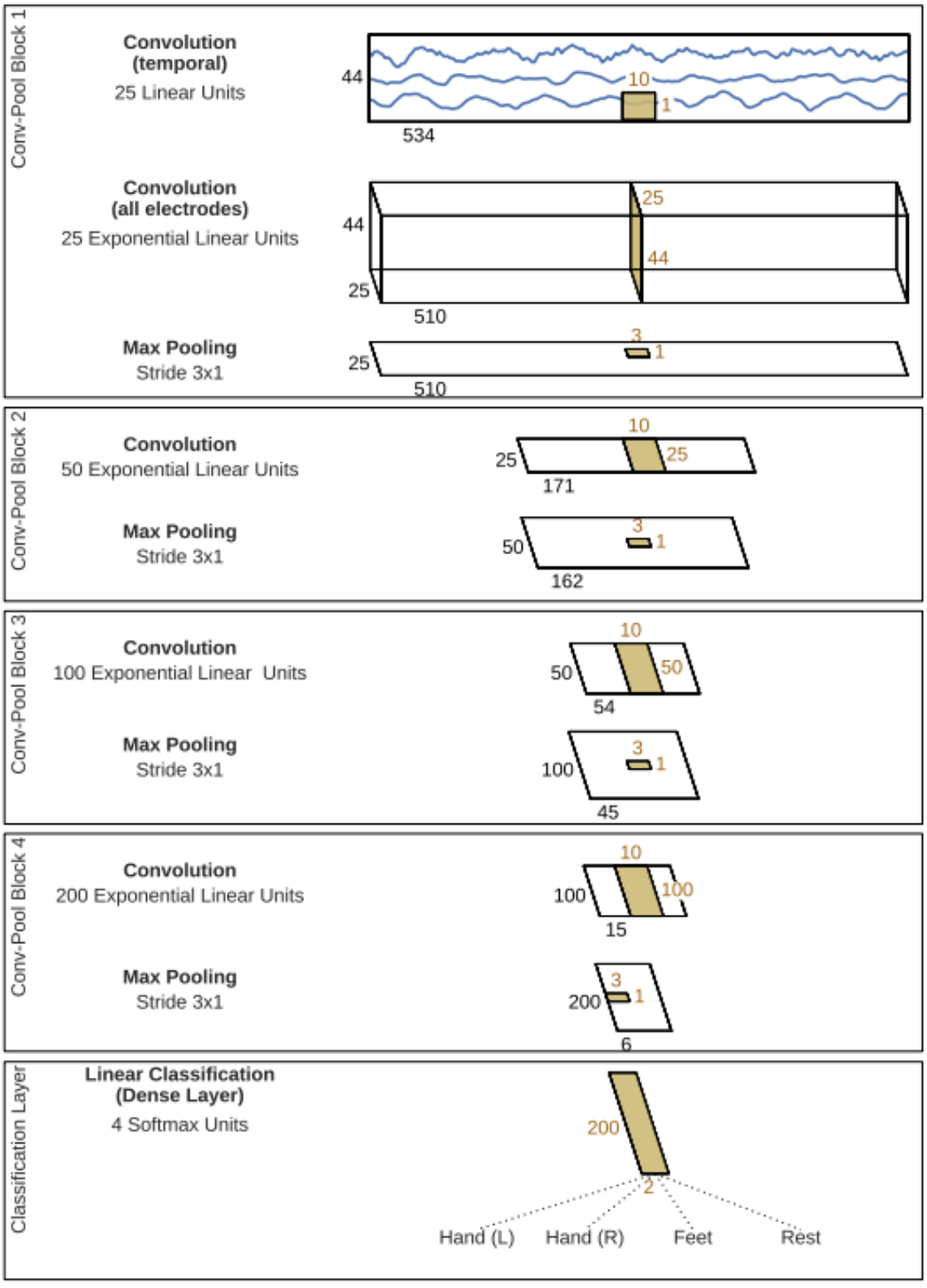

FIGURE 3.16. The architecture of Deep ConvNet algorithm. Adapted from [5]

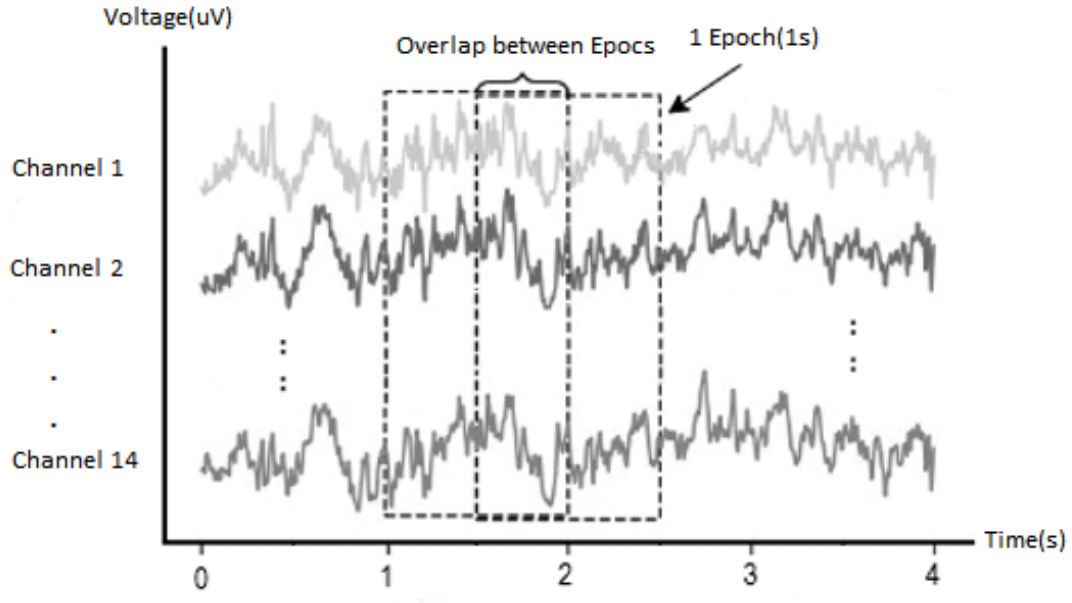

FIGURE 3.17. Preparation of time-series EEG Data input for the proposed models

tagged with the label of the main data. The VE created using the factors of navigation speed, scene complexity, and stereoscopic rendering parameters induced cybersickness in different severity. For example, most of the participants did not experience cybersickness in most of the navigation speed levels, except for very high speeds. In contrast, most of the participants experienced cybersickness in the majority of the scenes created using different stereoscopic rendering parameters. This makes it inevitable to augment the data in case of class imbalance to make a proper classification. Therefore, 50% overlap is preferred between the consecutive steps of the sliding window, while the data corresponding to the cybersickness condition are divided into pieces. On the other hand, training data were partitioned without overlapping in stereoscopic rendering parameters originated cybersickness data, 75% of overlap in speed originated cybersickness data, 25% of overlap in complexity originated cybersickness data in the factor type classification model. Finally, partitioned, augmented, and labeled data were scaled by the min-max of the current chunk.

Chapter 4.

Results

The decoding performances of the cybersickness detection and factor type classification models were shared first. In the second part, the performance of the proposed cybersickness mitigation system was evaluated by analyzing the time-dependent changes in the cue parameters, general discomfort scores filled out after each session, and the SSQ score differences filled out before and after each session in the feedback phase experiment.

4.1. Training Results of the Cybersickness Detection and the Factor Type Classification Models

The participants were presented with cues to induce different levels of cybersickness, and then the corresponding EEG data were labeled according to general discomfort scores collected from participants after each cue. Two Shallow ConvNet models based on the FBCSP algorithm were trained with labeled data collected in the training phase. The Shallow ConvNet architecture shows outstanding performance on the oscillatory signal classification. The classification accuracy of the Shallow ConvNet architecture evaluated against the EEGNet and the DeepConvNet algorithms, which yielded state-of-art decoding accuracy, especially for the motor imaginary task classification.

For performance analysis, we use five-fold cross-validation, where 20% of the total data were used as the test set, 10% of the remaining data as the validation set, and the remaining data as

TABLE 4.1. Decoding accuracies of the cybersickness detection models. Accuracy was calculated by averaging the overall accuracies obtained with 5-fold cross validation training.

	EEGNET4.2	EEGNET8.2	Deep ConvNet	Shallow ConvNet
Accuracy	63.9%	64.8%	69.01%	76.26%

TABLE 4.2. Decoding accuracies of the factor type classification models. Convention as in Table 4.1.

	EEGNET4.2	EEGNET8.2	Deep ConvNet	Shallow ConvNet
Accuracy	53.5%	64.5%	72.8%	81.01%

TABLE 4.3. Statistical report for the cybersickness detection model. Metrics were calculated by averaging the all results obtained with 5-fold cross validation training.

	precision	recall	f1-score
Comfortable	0.77	0.67	0.72
Uncomfortable	0.76	0.84	0.80
Overall Accuracy	76.26		

the training set. The average performances of the models were evaluated based on precision, recall, and F-measures metrics. Precision is defined as the metric that indicates success in a situation estimated positively. Recall shows how successfully positive states are predicted. F-measure is the harmonic average of the precision and recall metrics.

The classification accuracies of the cybersickness detection and the factor type classification models across all mentioned algorithms are shown in Table 4.1. and Table 4.2., respectively. The comparison results clearly show that the Shallow ConvNet architecture outperforms all others in both models. Although this approach has a shallow architecture compared to other models, the reason it exhibited an outstanding performance is that it was designed specifically to extract log band power features.

The classification performances of both models averaged over five folds are shown in Table 4.3. and Table 4.4. in terms of precision, recall, and F-measures metrics. The confusion matrices are shown in Figure 4.1. and Figure 4.2. which show the percentage of correct and incorrect estimates of classification model as a table. The cybersickness detection model's performance reached an overall accuracy of 76.26%, while the factor type classification model achieved 81.01% overall accuracy. The classification precision of each factor type

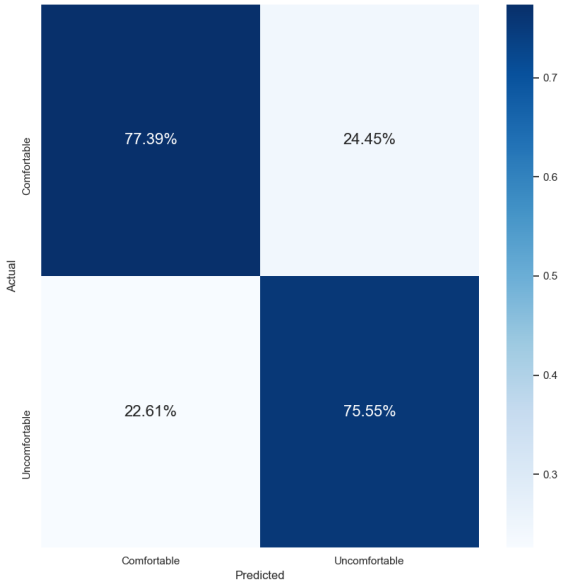

FIGURE 4.1. Confusion Matrix for the Cybersickness Detection Model

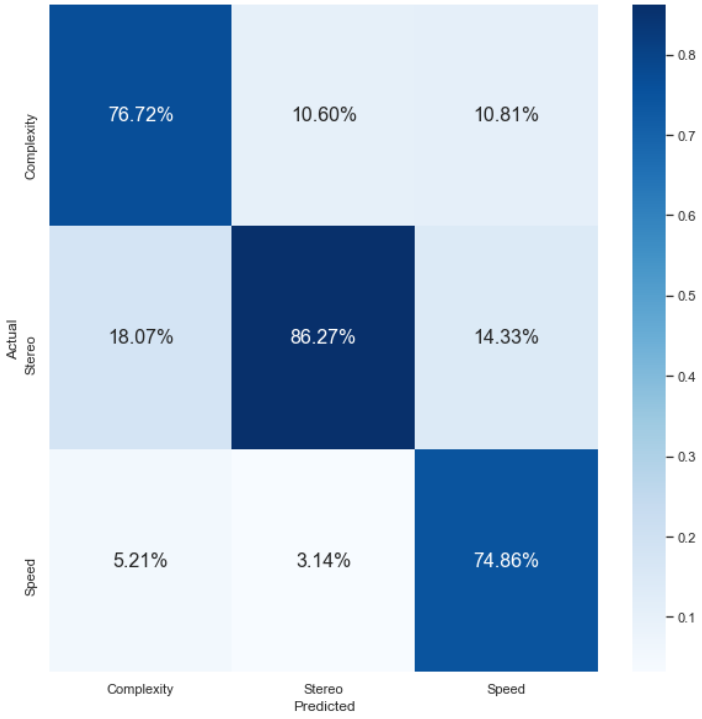

FIGURE 4.2. Confusion Matrix for the Factor Type Classification Model

TABLE 4.4. Statistical report for the factor type classification model. Convention as in Table 4.3.

	precision	recall	f1-score
Complexity	0.77	0.70	0.73
Stereo	0.86	0.84	0.85
Speed	0.75	0.87	0.80
Overall Accuracy	81.01		

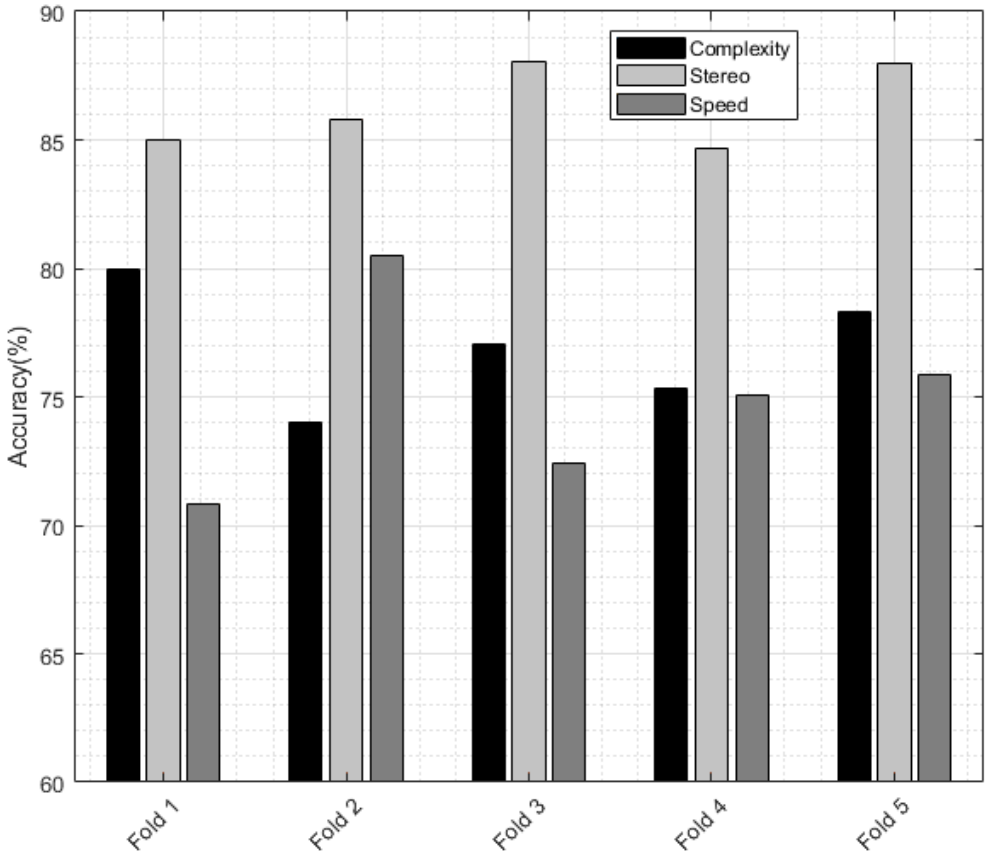

FIGURE 4.3. Plot illustrating precision of the factor type classification model for each class.

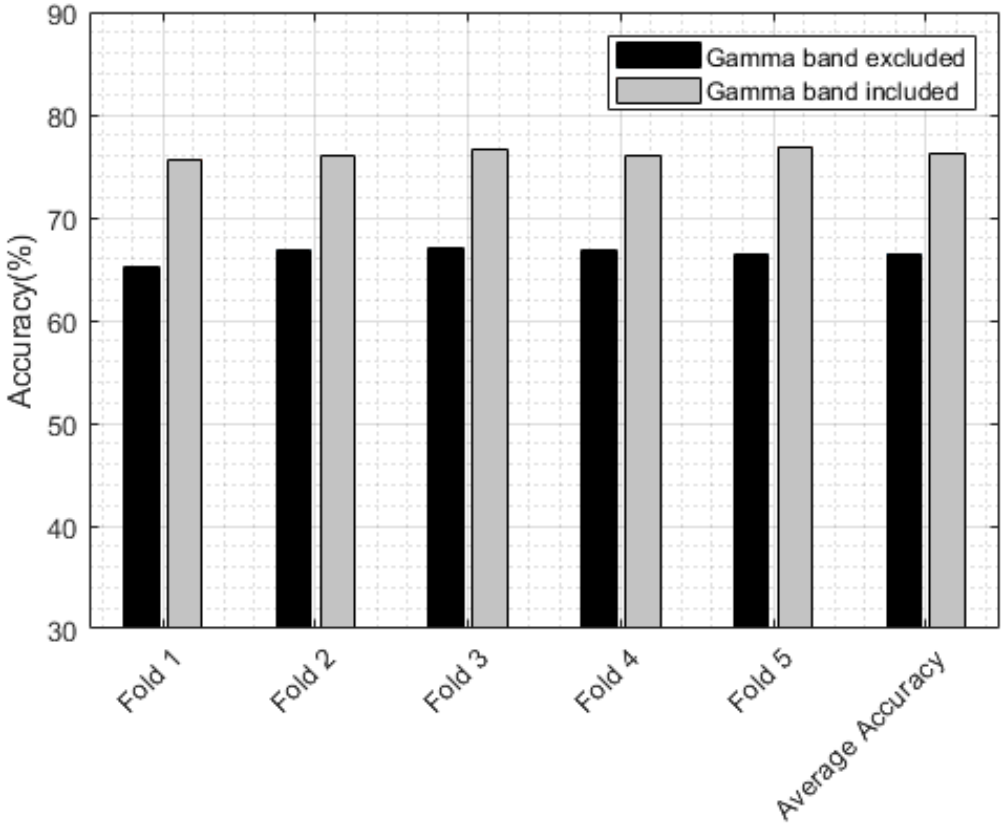

FIGURE 4.4. Decoding accuracies of the cybersickness detection model trained with EEG data excluding and including the gamma band

in the factor type classification model for each fold is given in Figure 4.3.. The results reveal that the precision of stereo class is superior to other classes in factor type classification. This situation is considered to be due to class imbalance that cannot be wholly eliminated even though we have used different rates of overlap between consecutive steps of the sliding window for each class.

One of the most critical steps in the classification of oscillatory EEG signals is to determine the operational frequency band based on the activity to be detected. Chuang et al. demonstrated that reported levels of motion sickness were positively correlated with gamma and alpha bands' activation [59]. Khaitami et al. investigated the relationship between cybersickness and gamma-band deviation [60]. The results showed an increase in gamma deviation in the EEG signal compared to the baseline when participants immersed in a VE.

The raw EEG data used in the training of the proposed models were filtered to include the

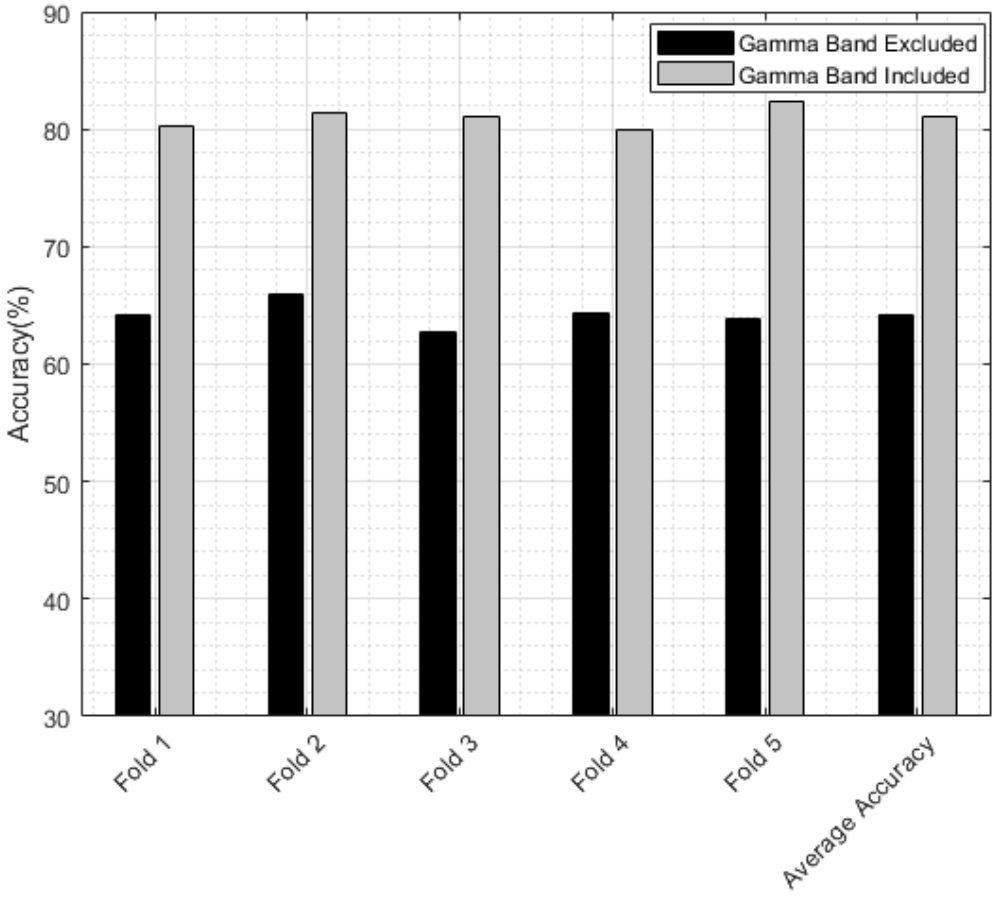

FIGURE 4.5. Decoding accuracies of the factor type classification model trained with EEG data excluding and including the gamma band

gamma band. The models were re-trained, excluding the gamma band, and classification performances of both cases were compared to show the correlation between cybersickness and the gamma band. The results revealed that the inclusion of the gamma band in the model input enables better EEG decoding accuracy consistent with the results unveiled in the referenced articles [59, 60]. The decoding accuracies of the cybersickness detection model trained with EEG data excluding and including the gamma band are shown in Figure 4.4.. The cybersickness detection model trained with EEG data, including the gamma band, performed better decoding accuracies in each fold and overall average results. A similar phenomenon is valid for the multi-class model in which the type of cue that causes cybersickness is classified. The model in which the gamma band was included in the input set achieved better performance than the model in which it was not included, as shown in Figure 4.5..

TABLE 4.5. The table present average of the changes in SSQ subscores and GDS score per session along with the RMANOVA test results

	Control 1 Session (M ± SD)	**Control 2 Session (M ± SD)**	**MIL Session (M ± SD)**	**Significance**
Change in SSQ-N Score	25.2 ± 8.8	46 ± 8.4	19.6 ± 6.2	$F_{2,32}$ = 125.209 $p < .001$
Change is SSQ-O Score	42.3 ± 21.2	78.4 ± 18.7	32.5 ± 6.9	$F_{2,32}$ = 82.447 $p < .001$
Change in SSQ-D Score	35.2 ± 17.1	67.1 ± 21.5	19.6 ± 9.9	$F_{2,32}$ = 56.485 $p < .001$
Change in SSQ-T Score	40.2 ± 13.1	74.8 ± 16.1	29 ± 5.6	$F_{2,32}$ = 111.331 $p < .001$
General Discomfort Score	3.8 ± 0.8	5.3 ± 1.1	3 ± 0.7	$F_{2,32}$ = 97.567 $p < .001$

4.2. Online Test Results

In the feedback phase, an experiment consisting of two control sessions, and one models-in-the-loop session was conducted with different participants to evaluate the performance of the proposed cybersickness detection and mitigation system. Performance of the proposed system was evaluated by using the differences of SSQ scores filled out at the beginning and the end of each session, the overall discomfort level scores rated after each session, and time-dependent changes in the cue parameters that were recorded in the session in which the proposed models were in-the-loop. Three of the participants did not experience cybersickness in any of the sessions, as shown in Figure 4.6.. Therefore, the results of the participants who did not experience cybersickness were analyzed separately from other participants to evaluate the performance of the proposed system in case the cybersickness is not experienced.

The statistical analyses of the feedback phase experiment were performed using the JASP tool [61] to evaluate the performance of the proposed cybersickness detection and mitigation system. Changes in the SSQ scores were taken into account to compare experienced cybersickness level between sessions. This approach aims to eliminate different initial states of participants as much as possible and isolate the effect of the stimulus shown. The SSQ response gives out a total SSQ score (SSQ-T) in addition to three different sub-scores in nausea (SSQ-N), disorientation (SSQ-D), and oculomotor discomfort (SSQ-O). The average values for change in SSQ scores and general discomfort level scores for each session are

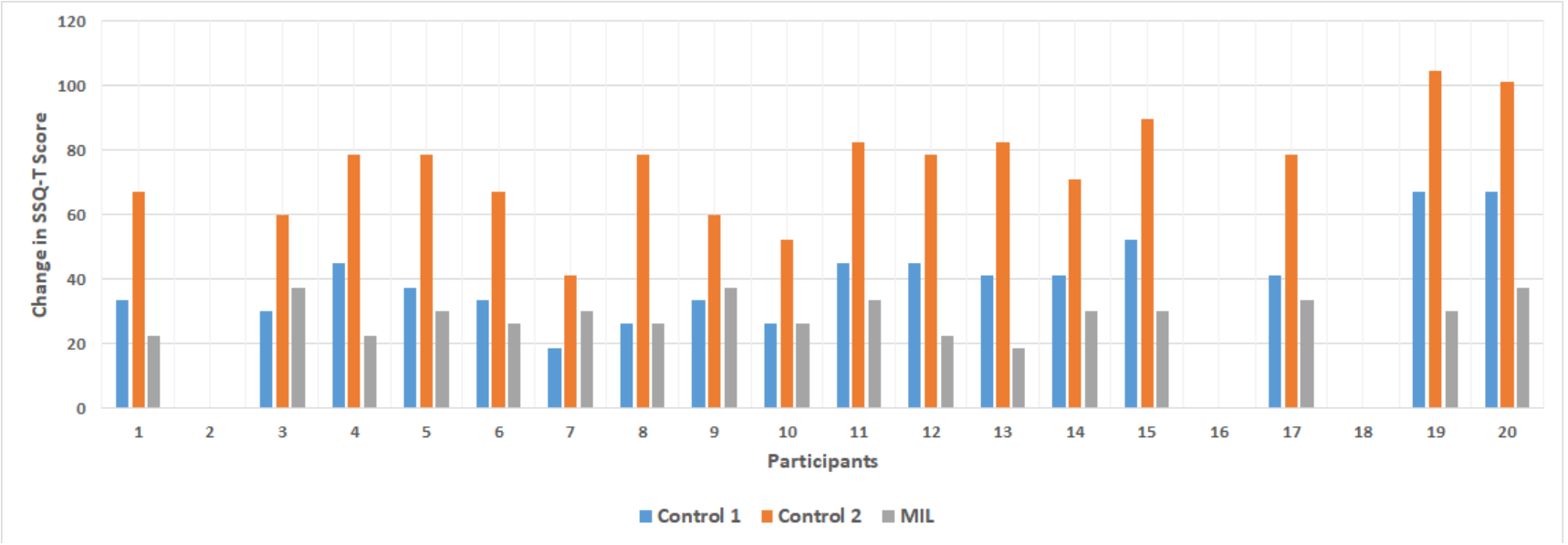

FIGURE 4.6. Plot illustrating the changes in SSQ-Total scores for all participants in each session.

FIGURE 4.7. Plot showing the min, max, and average values for the change in SSQ scores and general discomfort level over participants who experience cybersickness.

TABLE 4.6. The table present the results of the Holm post hoc test, which allows to discover which specific session differed.

	Post Hoc Tests			
			t	p_{holm}
SSQ-N	Control 1 Session (M=25.2, SD=8.9)	Control 2 Session	-11.824	.001
		Models-in-the-loop Session	3.196	0.003
	Control 2 Session (M=46, SD=8.4)	Models-in-the-loop Session (M= 19.6, SD=6.3)	15.020	.001
SSQ-O	Control 1 Session (M=42.4, SD=12.3)	Control 2 Session	-9.588	.001
		Models-in-the-loop Session	2.604	0.014
	Control 2 Session (M=78.5, SD=18.8)	Models-in-the-loop Session (M= 32.6, SD=6.9)	12.192	.001
SSQ-D	Control 1 Session (M=35.2, SD=17.1)	Control 2 Session	-7.009	.001
		Models-in-the-loop Session	3.415	0.002
	Control 2 Session (M=67.1, SD=21.6)	Models-in-the-loop Session (M= 19.6, SD=9.9)	10.424	.001
SSQ-T	Control 1 Session (M=40.2, SD=13.2)	Control 2 Session	-10.805	.001
		Models-in-the-loop Session	3.510	0.001
	Control 2 Session (M=74.8, SD=16.2)	Models-in-the-loop Session (M= 29, SD=5.7)	14.315	.001
General Discomfort Score	Control 1 Session (M=3.8, SD=0.8)	Control 2 Session	-9.145	.001
		Models-in-the-loop Session	4.572	.001
	Control 2 Session (M=5.3, SD=1.1)	Models-in-the-loop Session (M=3.1, SD=0.8)	13.717	.001

shown in Figure 4.7.. The average scores indicate that more cybersickness was induced to the participants in the control 2 session as expected. Besides, in the session in which the proposed cybersickness detection and mitigation system was utilized, the participants felt less cybersickness than both control sessions. To investigate results further, changes in all SSQ scores and general discomfort level scores were subject to a one way repeated measures analysis of variance (RMANOVA) test. A one-way repeated measures ANOVA was conducted to compare the level of experienced cybersickness for the control 1, control 2, and the MIL sessions. The RMANOVA rejected the null hypothesis for all scores, as shown in Table 4.5., which means that there is a significant difference between three sessions for all scores, but the results do not inform which of the various pairs of session the difference is significant. Therefore, a post hoc test was applied to investigate pairwise comparisons between the three sessions using the Holm correction for all scores. The results of the post hoc pairwise comparisons using the Holm correction are shown in Table 4.6.. A post hoc pairwise comparison

using the Holm correction revealed:

- Post Hoc Test Results for SSQ-N
  - There was a significant difference between the Control 1 Session (M=25.2, SD=8.9) and the Control 2 Session (M=46, SD=8.4); t=-11.824, p$<$.001.
  - There was a significant difference between the Control 1 Session and the Models-in-the-loop Session (M= 19.6, SD=6.3); t=3.196, p=0.003.
  - There was a significant difference between the Control 2 Session and the Models-in-the-loop Session; t=15.020, p$<$.001.
- Post Hoc Test Results for SSQ-O
  - There was a significant difference between the Control 1 Session (M=42.4, SD=12.3) and the Control 2 Session (M=78.5, SD=18.8); t=-9.588, p$<$.001.
  - There was a significant difference between the Control 1 Session and the Models-in-the-loop Session (M= 32.6, SD=6.9); t=2.604, p=0.014.
  - There was a significant difference between the Control 2 Session and the Models-in-the-loop Session; t=12.192, p$<$.001.
- Post Hoc Test Results for SSQ-D
  - There was a significant difference between the Control 1 Session (M=35.2, SD=17.1) and the Control 2 Session (M=67.1, SD=21.6); t=-7.009, p$<$.001.
  - There was a significant difference between the Control 1 Session and the Models-in-the-loop Session (M= 19.6, SD=9.9); t=3.415, p=0.002.
  - There was a significant difference between the Control 2 Session and the Models-in-the-loop Session; t=10.424, p$<$.001.
- Post Hoc Test Results for SSQ-T
  - There was a significant difference between the Control 1 Session (M=40.2, SD=13.2) and the Control 2 Session (M=74.8, SD=16.2); t=-10.805, p$<$.001.
  - There was a significant difference between the Control 1 Session and the Models-in-the-loop Session (M= 29, SD=5.7); t=3.510, p=0.001.

  - There was a significant difference between the Control 2 Session and the Models-in-the-loop Session; t=14.315, p<.001.

- Post Hoc Test Results for GDS
  - There was a significant difference between the Control 1 Session (M=3.8, SD=0.8) and the Control 2 Session (M=5.3, SD=1.1); t=-9.145, p<.001.
  - There was a significant difference between the Control 1 Session and the Models-in-the-loop Session (M= 3.1, SD=0.8); t=4.572, p<.001.
  - There was a significant difference between the Control 2 Session and the Models-in-the-loop Session; t=13.717, p<.001.

In addition to questionnaire scores, time-dependent changes in the cue parameters were recorded for all users in the models-in-the-loop session. The time-dependent changes in the cue parameters used to create the virtual scene is shown in Figure 4.8. for each participant separately. The individual results of the time-dependent changes in the cue parameters revealed that the levels of experienced cybersickness and the factors caused discomfort differed significantly among the participants, and performing analyzes on personal results may not give an inclusive implication. Therefore, averages of time-series cue parameters over participants who experienced cybersickness were taken under consideration to evaluate the overall performance of the CDMS. The time-dependent changes in averaged cue parameters over participants who experienced cybersickness are shown in Figure 4.9.. The results revealed that updates were mostly made in the stereoscopic rendering parameters and at least in the navigation speed parameter following the feedback from the proposed mitigation system. This also means that experienced cybersickness was mostly caused by stereoscopic rendering parameters and at least the navigation speed. The cue parameters were initiated to induce a moderate level of cybersickness in all sessions. Therefore, some participants began to experience cybersickness after the session started, and the proposed mitigation system started to update the relevant parameters for a more comfortable vision. This situation caused the complexity and stereoscopic rendering parameters not to reach the levels to induce the most severe cybersickness, unlike the control 1 and control 2 sessions. These results are consistent with the findings of the lowest severe cybersickness experienced in the MIL session, which was revealed in the analysis of change in SSQ and general discomfort level scores.

The SSQ scores of participants, who did not feel cybersickness in any of the sessions, are zero, and the general discomfort levels are 1 out of 7. The time-dependent changes in the

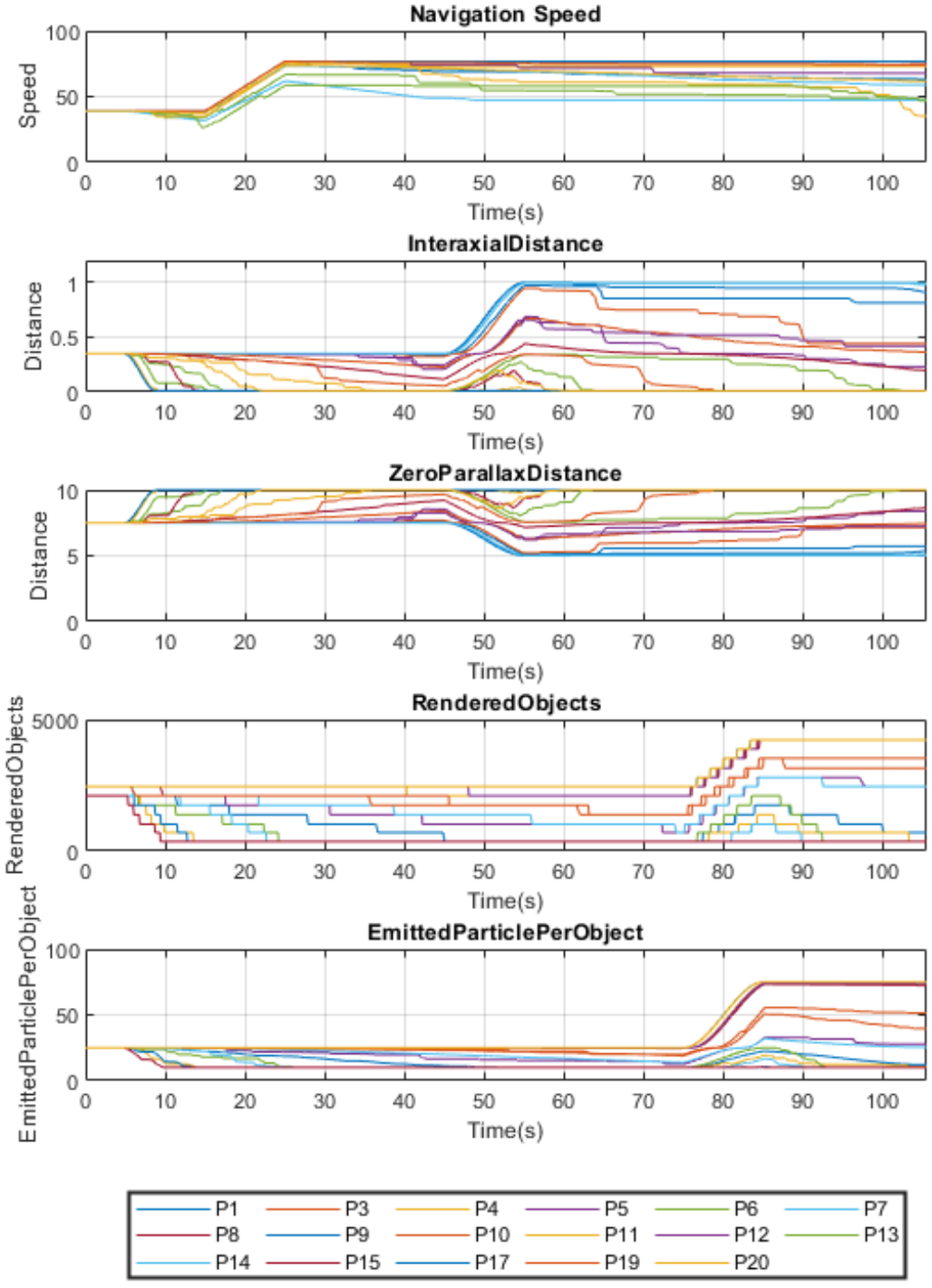

FIGURE 4.8. Plots showing the change in the cue parameters for each participants who experience cybersickness

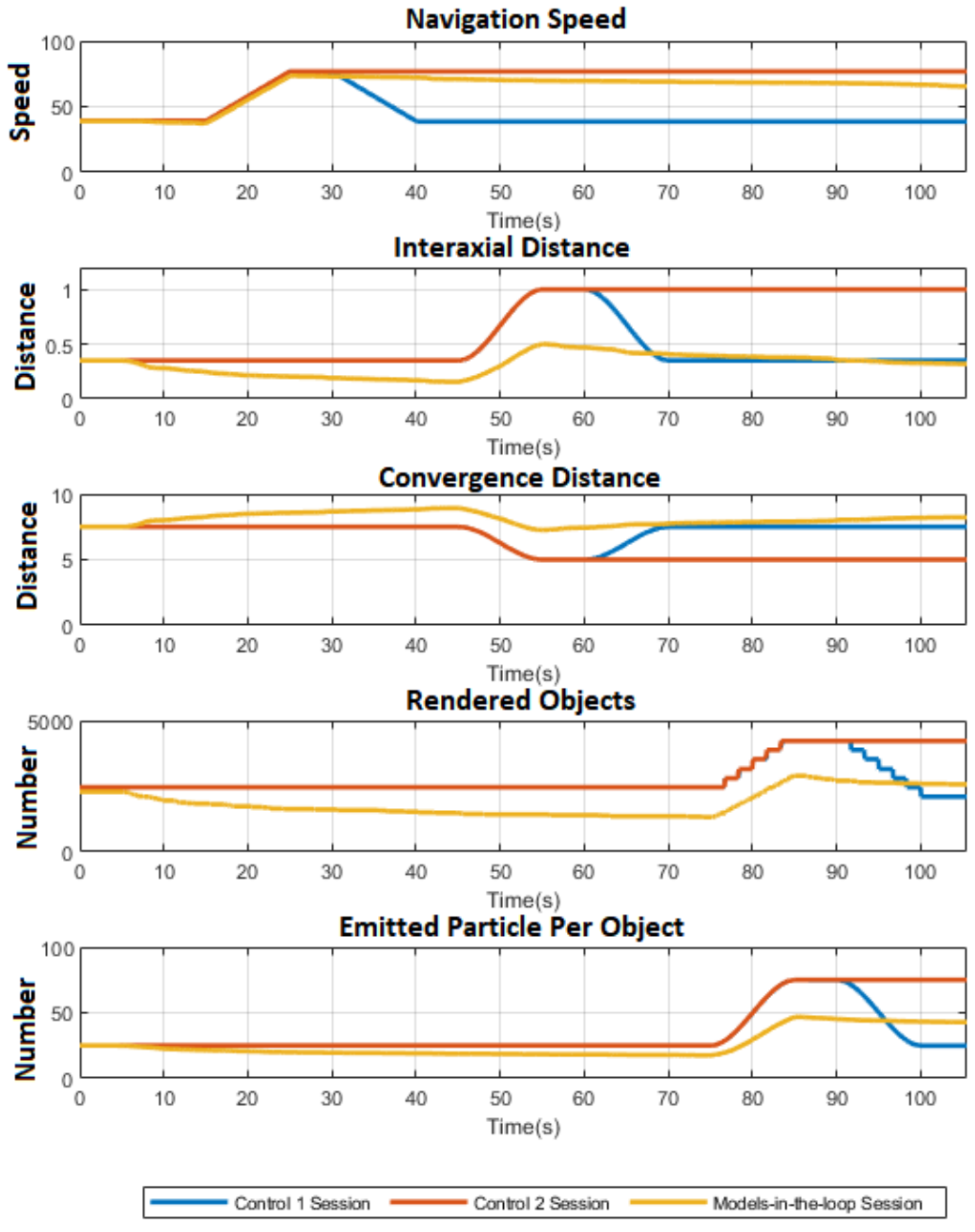

FIGURE 4.9. Plots showing the change in the cue parameters averaged over participants who experience cybersickness

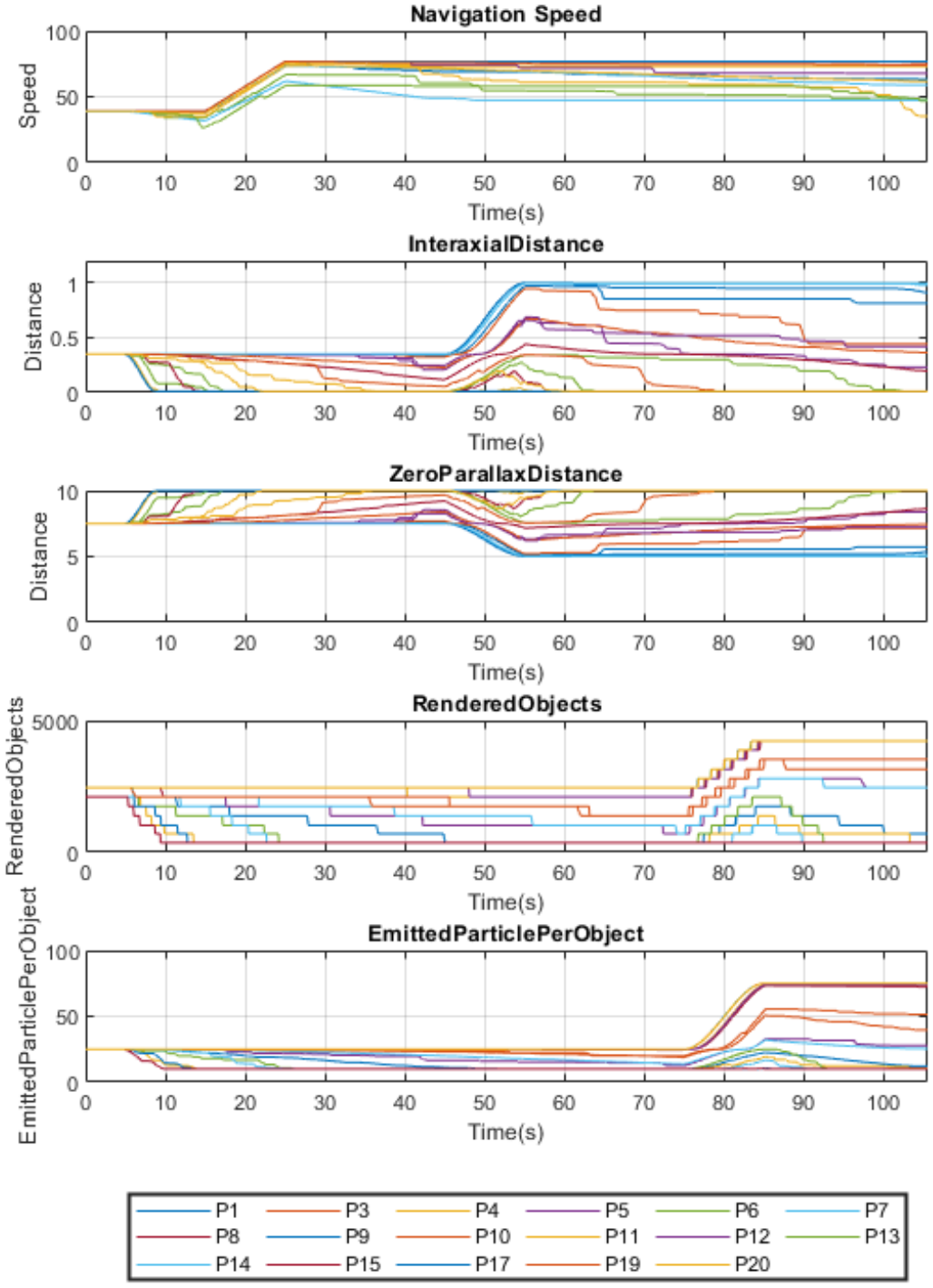

FIGURE 4.10. Plots showing the change in the cue parameters for each participants who didn't experience cybersickness

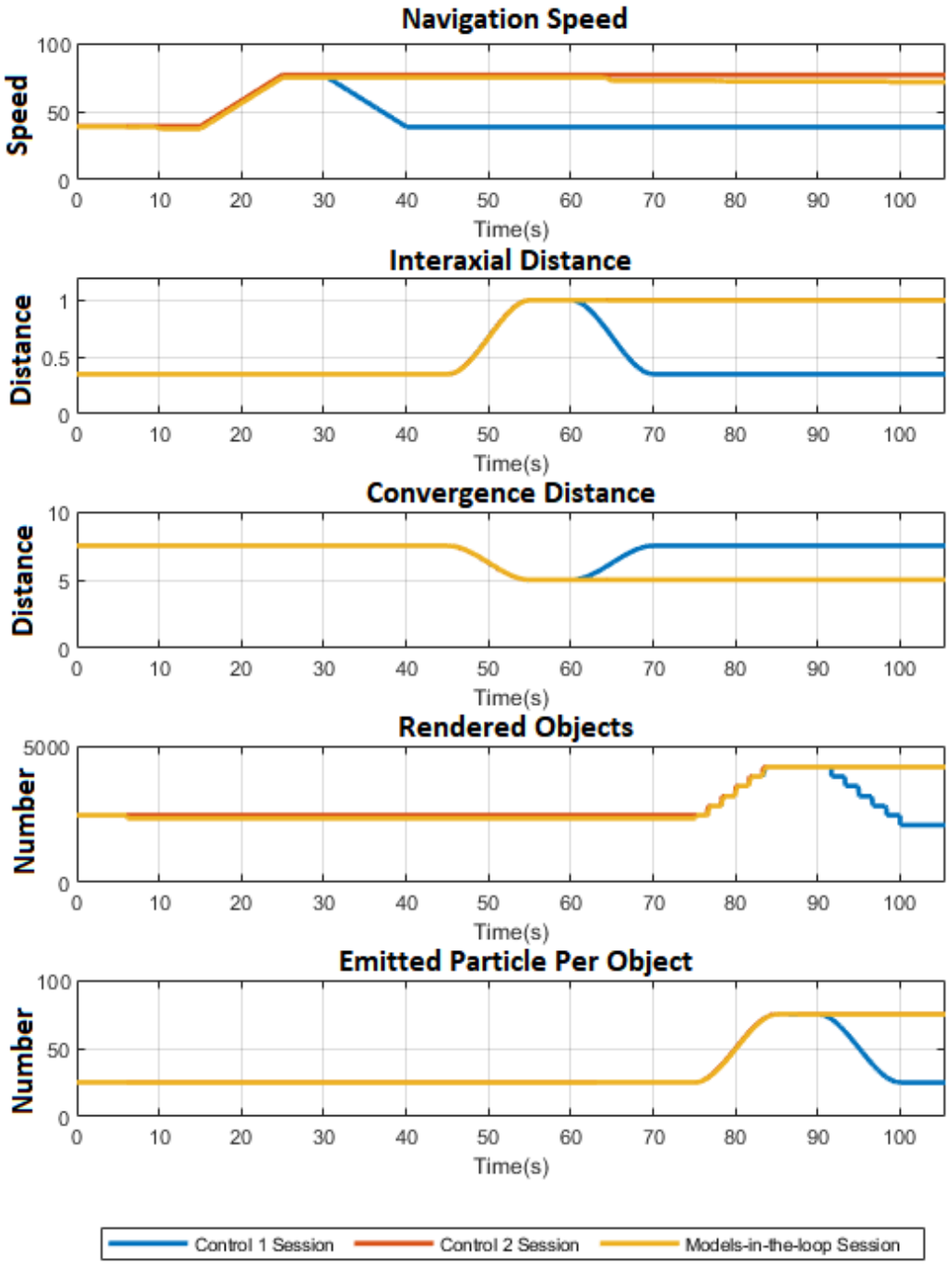

FIGURE 4.11. Plots showing the change in the cue parameters averaged over participants who didn't experience cybersickness

cue parameters used to create the virtual scene is shown in Figure 4.10. for each participant separately. The averages of the time-series cue parameters over these participants are shown in Figure 4.11.. Changes in the cue parameters reveal that despite the few stages of updates that may be neglected, the parameters were not significantly interfered with. This shows that the proposed model preserves the presented scene by making the correct classification even when cybersickness is not experienced.

Chapter 5.

Discussion and Conclusion

5.1. Discussion

Various factors that cause cybersickness have been investigated in the literature. In this study, navigation speed, scene complexity, and stereoscopic rendering parameters were examined as cybersickness factors. In the first phase of the study, the two-stage models were trained to detect cybersickness and to classify the factor type, causing cybersickness. EEG data fed to the proposed models were collected from participants immersed in the VE where the specified factors were simulated. In the second phase, the performance of the cybersickness detection and mitigation system was evaluated by conducting an experiment with the participants who did not participate in the first phase experiment.

The cybersickness experienced in a VE is in the type of oscillatory activities. These are observed as asynchronous power changes in the specific frequency band after a cumulative effect, as opposed to the activities in which the response is seen after a certain time as a result of a given stimulus. Therefore, in this study, the Shallow ConvNet model based on the FBCSP algorithm, which shows outstanding performance in the detection of oscillatory activities, was used to detect cybersickness and to classify the factor causing cybersickness. We reached the decoding accuracy of 76.26% in the cybersickness detection model. We showed that the inclusion of the gamma band in the training data increases accuracy from 66.52% to 76.26%. Besides, the classification accuracy of the cybersickness detection model

was evaluated against the EEGNet and the DeepConvNet algorithms. The cybersickness detection model performed significantly better than specified algorithms. The factor type classification model with similar architecture was trained using data collected only in situations in which cybersickness was experienced. The performance of the factor type classification model reached up to an overall accuracy of 81.01%. The proposed model outperformed all specified alternatives by a significant margin. Similar to the first model, the inclusion of the gamma band in the input set had significantly increased the decoding performance of the factor type classification model. The factor type classification model's precision results revealed that the stereo class's precision outperforms all others in each fold result. This is considered to be due to the class imbalance that cannot be eliminated completely, although different rates of overlap were used for each class data between consecutive steps of sliding window.

The cybersickness detection and mitigation system's performance was evaluated by an online experiment consisting of three consecutive sessions. The online experiment was carried out with 20 participants who did not participate in the experiment carried out in the first phase. The participants had similar VR experience, age average, game habit, and the MMSQ percentile with the participants of the feedback phase experiment. In the online experiment, the participants were immersed in the VE where the cue parameters shifted according to specific templates in control 1 and control 2 sessions. In the session in which the trained models were in the loop, the cue parameters were updated according to feedback from the factor type classification model. The changes in the SSQ scores collected at the beginning and the end of each session and the general discomfort level scores rated after all sessions revealed that, on average, users experienced the most severe cybersickness in the control 2 session, and the least discomfort in the session in which the proposed models were utilized. The changes in the SSQ scores and general discomfort scores were subject to a one way repeated measures analysis of variance (RMANOVA) test. The RMANOVA rejected the null hypothesis for all SSQ subscores, SSQ total score, and general discomfort score. Post hoc tests using the Holm correction revealed that there is a significant difference between the three sessions for all scores.

Time-dependent changes in the cue parameters showed that cybersickness caused by complexity predominated in some users, while in others, the cybersickness was caused by stereoscopic rendering parameters. It was also revealed that the participants experienced navigation

speed-related cybersickness less than other factors-related discomforts. The results were expected to vary across users due to different individual tolerances to the cybersickness and non-stationary characteristics of the measured EEG data. Therefore, it is more accurate to make the performance evaluation of the CDMS according to the changes in the cue parameters averaged over all participants. The average results showed that the cue parameters were updated by the CDMS so that the complexity and stereoscopic rendering parameters did not reach the most severe cybersickness induction levels, and at the end of the session, they reached moderate levels similar to those of the control 1 session. There was little intervention in the navigation speed parameter before reaching the level where it would induce maximum cybersickness, and then it was gradually reduced in line with the feedback received. These results are consistent with the findings revealed in the comparison of the SSQ and general discomfort scores between sessions that the least cybersickness was experienced in the MIL session. Besides, the averages of the time-dependent changes in the cue parameters over the participants who did not experience cybersickness in any session showed that the CDMS made the cybersickness detection with high accuracy and without offsetting cybersickness condition.

The correlation between the MSSQ percentiles, change in the SSQ-T score, general discomfort scores, and averaged cue parameters over the MIL session are demonstrated in Figure 5.1. for all participants. The cue parameters were updated following the discomfort experienced by the participants. The low value of the convergence distance parameter and the high values of the remaining cue parameters indicate that the user experienced less cybersickness, and therefore, the cue parameters were less modified. In other words, the cue parameters of users with low SSQ-T score changes remain at higher value since they are updated less frequently. This is consistent with the finding that change in the SSQ-T score shows a positive correlation with convergence distance and negative correlation with interaxial distance, particle rate over time, and rendered objects parameters. Besides, the low correlation between change in the SSQ-T score and the navigation speed is consistent with the finding of the training phase that the participants experienced less speed-related cybersickness. The high negative correlation between the MSSQ score and the navigation speed showed that the MSSQ is a suitable measurement method for the evaluation of navigation speed-related cybersickness experienced in a VE. Lastly, a high positive correlation between change in the SSQ-T score and the single-question general disturbance query score shows that single-question surveys, in which the user was less disturbed during the filling out period, are an efficient measure for assessing cybersickness severity.

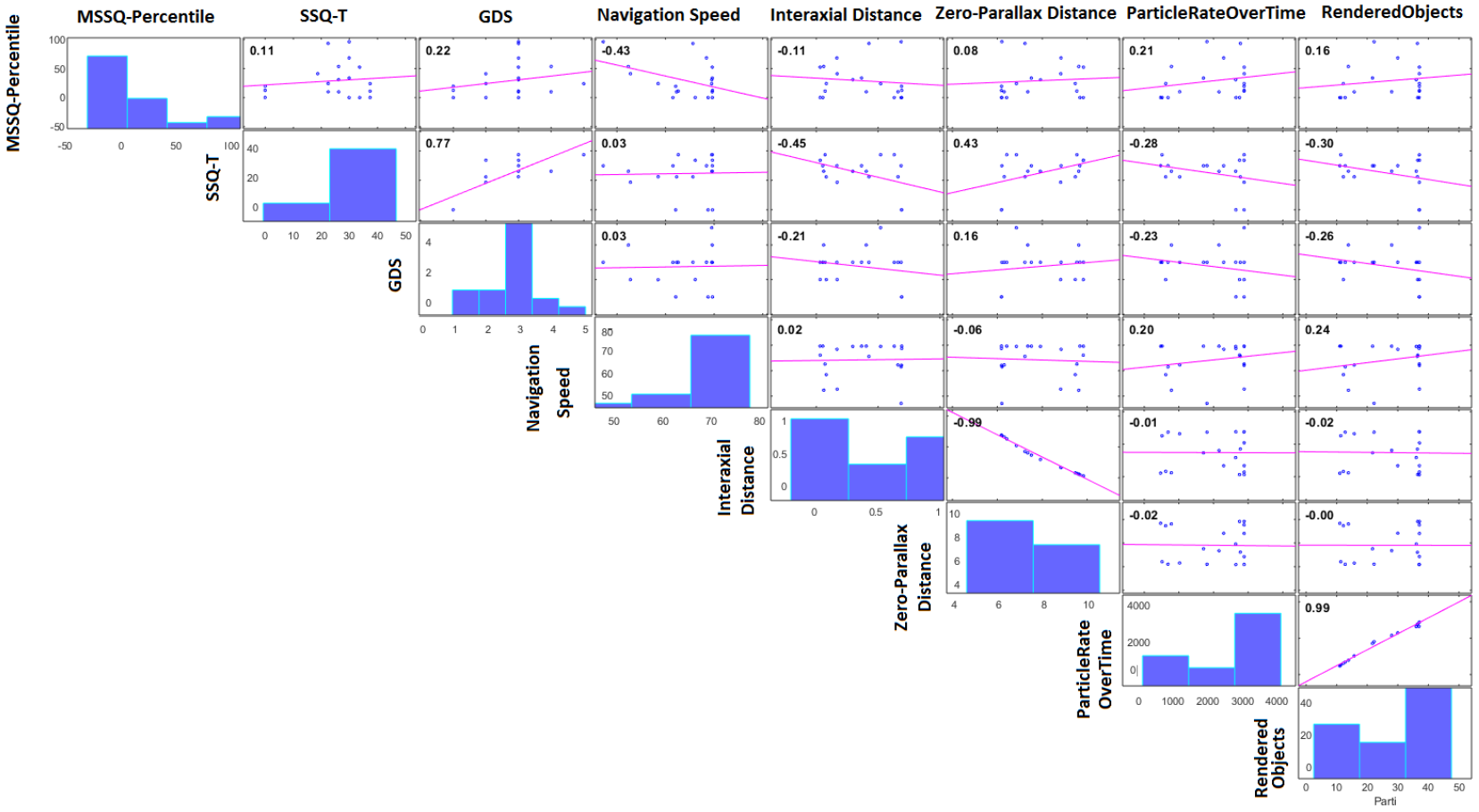

FIGURE 5.1. Plots showing the correlation between MSSQ percentiles, SSQ-T score difference, general discomfort score, and averaged cue parameters over the models-in-the-loop session

5.2. Conclusion

In this study, we propose a novel system that enables the simultaneous detection and mitigation of the cybersickness experienced by users immersed in a VE. Cybersickness can be caused by various factors, which are generally categorized as an individual, hardware, and software-related factors. In this study, we simulated navigation speed, scene complexity, and stereoscopic rendering parameters as software-related factors, which are widely used in cybersickness studies and whose effect has been confirmed. Two Shallow ConvNet models based on the FBCSP algorithm were trained using the EEG data collected from 33 participants in the training phase. In the first model, experienced cybersickness is detected, and in the second model, the factor causing cybersickness is classified. The experiment conducted in the feedback phase consists of three consecutive sessions. The participants were subjected to two control sessions to evaluate the performance of the CDMS, along with the session in which the proposed cybersickness detection and mitigation system was utilized. To evaluate the performance of the CDMS on different users without individual calibration, 20 users who did not participate in the training phase were included in the feedback phase experiment. The findings revealed in the comparison of SSQ, and general discomfort scores between sessions and the time-dependent changes in cue parameters in the MIL session show the outstanding performance of the CDMS despite the challenge of cross-subject variability in the experiment.

REFERENCES

[1] Emotiv epoc+. https://www.emotiv.com/epoc/. Accessed: 2019-11-19.

[2] J.G. Betts, P. Desaix, E.W. Johnson, J.E. Johnson, O. Korol, D. Kruse, B. Poe, OpenStax College, J. Wise, M.D. Womble, et al. *Anatomy & Physiology*. Open Textbook Library. OpenStax College, Rice University, **2013**. ISBN 9781938168130.

[3] Kai Keng Ang, Zheng Yang Chin, Haihong Zhang, and Cuntai Guan. Filter bank common spatial pattern (fbcsp) in brain-computer interface. In *2008 IEEE International Joint Conference on Neural Networks (IEEE World Congress on Computational Intelligence)*, pages 2390–2397. **2008**. ISSN 2161-4407. doi: 10.1109/IJCNN.2008.4634130.

[4] Vernon J Lawhern, Amelia J Solon, Nicholas R Waytowich, Stephen M Gordon, Chou P Hung, and Brent J Lance. Eegnet: a compact convolutional neural network for eeg-based brain–computer interfaces. *Journal of Neural Engineering*, 15(5):056013, **2018**. ISSN 1741-2552. doi:10.1088/1741-2552/aace8c.

[5] Robin Tibor Schirrmeister, Jost Tobias Springenberg, Lukas Dominique Josef Fiederer, Martin Glasstetter, Katharina Eggensperger, Michael Tangermann, Frank Hutter, Wolfram Burgard, and Tonio Ball. Deep learning with convolutional neural networks for eeg decoding and visualization. *Human Brain Mapping*, 38(11):5391–5420, **2017**. ISSN 1065-9471. doi:10.1002/hbm.23730.

[6] Yi-Chou Chen, Xiao Dong, Jens Hagstrom, and Thomas Stoffregen. Control of a virtual ambulation influences body movement and motion sickness. *BIO Web of Conferences*, 1:00016, **2011**. doi:10.1051/bioconf/20110100016.

[7] Young Kim, Hyun Kim, Eun Kim, Hee Ko, and Hyun-Taek Kim. Characteristic changes in the physiological components of cybersickness. *Psychophysiology*, 42:616–25, **2005**. doi:10.1111/j.1469-8986.2005.00349.x.

[8] Paul DiZio and James R. Lackner. Circumventing side effects of immersive virtual environments. In *HCI*. **1997**.

[9] Mark Mon-Williams, John Wann, and Simon Rushton. Design factors in stereoscopic virtual-reality displays. *Journal of The Society for Information Display - J SOC INF DISP*, 3, **1995**. doi:10.1889/1.1984970.

[10] Lisa Rebenitsch and Charles Owen. Review on cybersickness in applications and visual displays. *Virtual Reality*, 20(2):101–125, **2016**.

[11] Jelte E. Bos, Willem Bles, and Eric L. Groen. A theory on visually induced motion sickness. *Displays*, 29(2):47 – 57, **2008**. ISSN 0141-9382. doi:https://doi.org/10.1016/j.displa.2007.09.002. Health and Safety Aspects of Visual Displays.

[12] Marcos Allue, Ana Serrano, Manuel G. Bedia, and Belen Masia. Crossmodal Perception in Immersive Environments. In Alejandro Garcia-Alonso and Belen Masia, editors, *Spanish Computer Graphics Conference (CEIG)*. The Eurographics Association, **2016**. ISBN 978-3-03868-023-9. ISSN -. doi:10.2312/ceig.20161307.

[13] David M. Hoffman, Ahna R. Girshick, Kurt Akeley, and Martin S. Banks. Vergence–accommodation conflicts hinder visual performance and cause visual fatigue. *Journal of Vision*, 8(3):33–33, **2008**. ISSN 1534-7362. doi:10.1167/8.3.33.

[14] Andrei Sherstyuk and Andrei State. Dynamic eye convergence for head-mounted displays. pages 43–46. **2010**. doi:10.1145/1889863.1889869.

[15] Robert S Kennedy, Norman E Lane, Kevin S Berbaum, and Michael G Lilienthal. Simulator sickness questionnaire: An enhanced method for quantifying simulator sickness. *The international journal of aviation psychology*, 3(3):203–220, **1993**.

[16] Young Kim, Eun Kim, Min Jae Park, Kwang Park, Hee Ko, and Hyun-Taek Kim. The application of biosignal feedback for reducing cybersickness from exposure to a virtual environment. *Presence Teleoperators amp Virtual Environments*, 17:1–16, **2008**. doi:10.1162/pres.17.1.1.

[17] Eugenia M Kolasinski. Simulator sickness in virtual environments. Technical report, Army research Inst for the behavioral and social sciences Alexandria VA, **1995**.

[18] L. L. Arns and M. M. Cerney. The relationship between age and incidence of cybersickness among immersive environment users. In *IEEE Proceedings. VR*

2005. Virtual Reality, 2005., pages 267–268. **2005**. ISSN 2375-5334. doi:10.1109/VR.2005.1492788.

[19] George D. Park, R. Wade Allen, Dary Fiorentino, Theodore J. Rosenthal, and Marcia L. Cook. Simulator sickness scores according to symptom susceptibility, age, and gender for an older driver assessment study. *Proceedings of the Human Factors and Ergonomics Society Annual Meeting*, 50(26):2702–2706, **2006**. doi:10.1177/154193120605002607.

[20] Kay Stanney, Kelly Hale, Isabelina Nahmens, and Robert Kennedy. What to expect from immersive virtual environment exposure: Influences of gender, body mass index, and past experience. *Human factors*, 45:504–20, **2003**. doi:10.1518/hfes.45.3.504.27254.

[21] K.J Hill and Peter Howarth. Habituation to the side effects of immersion in a virtual environment. *Displays*, 21:25–30, **2000**. doi:10.1016/S0141-9382(00)00029-9.

[22] Peter Howarth and Simon Hodder. Characteristics of habituation to motion in a virtual environment. **2014**.

[23] Kay M. Stanney, D. Susan Lanham, Robert S. Kennedy, and Robert Breaux. Virtual environment exposure drop-out thresholds. *Proceedings of the Human Factors and Ergonomics Society Annual Meeting*, 43(22):1223–1227, **1999**. doi:10.1177/154193129904302212.

[24] Sarah Sharples, Sue Cobb, Amanda Moody, and John R. Wilson. Virtual reality induced symptoms and effects (vrise): Comparison of head mounted display (hmd), desktop and projection display systems. *Displays*, 29(2):58 – 69, **2008**. ISSN 0141-9382. doi:https://doi.org/10.1016/j.displa.2007.09.005. Health and Safety Aspects of Visual Displays.

[25] Caglar Yildirim. Cybersickness during vr gaming undermines game enjoyment: A mediation model. *Displays*, 59:35–43, **2019**.

[26] Andrej Somrak, Iztok Humar, M Shamim Hossain, Mohammed F Alhamid, M Anwar Hossain, and Jože Guna. Estimating vr sickness and user experience using different hmd technologies: An evaluation study. *Future Generation Computer Systems*, 94:302–316, **2019**.

[27] A.F. Seay, David Krum, Larry Hodges, and W. Ribarsky. Simulator sickness and presence in a high fov virtual environment. pages 299 – 300. **2001**. ISBN 0-7695-0948-7. doi:10.1109/VR.2001.913806.

[28] Henry Duh, James Lin, Robert Kenyon, Don Parker, and Thomas Furness. Effects of field of view on balance in immersive environment. pages 235–240. **2001**. ISBN 0-7695-0948-7. doi:10.1109/VR.2001.913791.

[29] R. H. Y. So, A. Ho, and W. T. Lo. A metric to quantify virtual scene movement for the study of cybersickness: Definition, implementation, and verification. *Presence*, 10(2):193–215, **2001**. ISSN 1054-7460. doi:10.1162/105474601750216803.

[30] Sunu Wibirama, Hanung A Nugroho, and Kazuhiko Hamamoto. Depth gaze and ecg based frequency dynamics during motion sickness in stereoscopic 3d movie. *Entertainment computing*, 26:117–127, **2018**.

[31] Behrang Keshavarz, Aaron Emile Philipp-Muller, Wanja Hemmerich, Bernhard E Riecke, and Jennifer L Campos. The effect of visual motion stimulus characteristics on vection and visually induced motion sickness. *Displays*, 58:71–81, **2019**.

[32] R. Welch, T. Blackmon, Andrew Liu, Barb Mellers, and L. Stark. The effects of pictorial realism. *Teleoperators and Virtual Environments - Presence*, **1996**.

[33] Beverly K Jaeger and Ronald R Mourant. Comparison of simulator sickness using static and dynamic walking simulators. In *Proceedings of the Human Factors and Ergonomics Society Annual Meeting*, volume 45, pages 1896–1900. SAGE Publications Sage CA: Los Angeles, CA, **2001**.

[34] Lorenzo Terenzi and Peter Zaal. Rotational and translational velocity and acceleration thresholds for the onset of cybersickness in virtual reality. In *AIAA Scitech 2020 Forum*, page 0171. **2020**.

[35] Eugenia Kolasinski and Richard Gilson. Simulator sickness and related findings in a virtual environment. *Proceedings of the Human Factors and Ergonomics Society Annual Meeting*, 42:1511–1515, **1998**. doi:10.1177/154193129804202110.

[36] Peter Alan Howarth. Oculomotor changes within virtual environments. *Applied Ergonomics*, 30(1):59 – 67, **1999**. ISSN 0003-6870. doi:https://doi.org/10.1016/S0003-6870(98)00043-X.

[37] EunHee Chang, InJae Hwang, Hyeonjin Jeon, Yeseul Chun, Hyun Taek Kim, and Changhoon Park. Effects of rest frames on cybersickness and oscillatory brain activity. In *2013 International Winter Workshop on Brain-Computer Interface (BCI)*, pages 62–64. IEEE, **2013**.

[38] Yu-Chieh Chen, Jeng-Ren Duann, Shang-Wen Chuang, Chun-Ling Lin, Li-Wei Ko, Tzyy-Ping Jung, and Chin-Teng Lin. Spatial and temporal eeg dynamics of motion sickness. *NeuroImage*, 49(3):2862–2870, **2010**.

[39] Min-Koo Kang, Hohyun Cho, Han-Mu Park, Sung Chan Jun, and Kuk-Jin Yoon. A wellness platform for stereoscopic 3d video systems using eeg-based visual discomfort evaluation technology. *Applied ergonomics*, 62:158–167, **2017**.

[40] Jasmin Kevric and Abdulhamit Subasi. Comparison of signal decomposition methods in classification of eeg signals for motor-imagery bci system. *Biomedical Signal Processing and Control*, 31, **2017**. doi:10.1016/j.bspc.2016.09.007.

[41] Xiu An, Deping Kuang, Xiaojiao Guo, Yilu Zhao, and Lianghua He. A deep learning method for classification of eeg data based on motor imagery. pages 203–210. **2014**. doi:10.1007/978-3-319-09330-7_25.

[42] Yousef Rezaeitabar and Ugur Halici. A novel deep learning approach for classification of eeg motor imagery signals. *Journal of Neural Engineering*, 14:016003, **2017**. doi:10.1088/1741-2560/14/1/016003.

[43] T. Wilaiprasitporn, A. Ditthapron, K. Matchaparn, T. Tongbuasirilai, N. Banluesombatkul, and E. Chuangsuwanich. Affective eeg-based person identification using the deep learning approach. *IEEE Transactions on Cognitive and Developmental Systems*, pages 1–1, **2019**. ISSN 2379-8939. doi:10.1109/TCDS.2019.2924648.

[44] Yilong Yang, Qingfeng Wu, Yazhen Fu, and Xiaowei Chen. Continuous convolutional neural network with 3d input for eeg-based emotion recognition. **2018**.

[45] Kai Keng Ang, Zheng Yang Chin, Chuanchu Wang, Cuntai Guan, and Haihong Zhang. Filter bank common spatial pattern algorithm on bci competition iv datasets 2a and 2b. *Frontiers in Neuroscience*, 6:39, **2012**. ISSN 1662-453X. doi:10.3389/fnins.2012.00039.

[46] Dalin Zhang, Lina Yao, Xiang Zhang, Sen Wang, Weitong Chen, and Robert Boots. Eeg-based intention recognition from spatio-temporal representations via cascade and parallel convolutional recurrent neural networks, **2017**.

[47] Pouya Bashivan, Irina Rish, M. Yeasin, and Noel Codella. Learning representations from eeg with deep recurrent-convolutional neural networks. **2015**.

[48] Daekyo Jeong, Sangbong Yoo, and Jang Yun. Cybersickness analysis with eeg using deep learning algorithms. pages 827–835. **2019**. doi:10.1109/VR.2019.8798334.

[49] J. Kim, W. Kim, H. Oh, S. Lee, and S. Lee. A deep cybersickness predictor based on brain signal analysis for virtual reality contents. In *2019 IEEE/CVF International Conference on Computer Vision (ICCV)*, pages 10579–10588. **2019**. ISSN 1550-5499. doi:10.1109/ICCV.2019.01068.

[50] Fabien Lotte. *A Tutorial on EEG Signal-processing Techniques for Mental-state Recognition in Brain–Computer Interfaces*, pages 133–161. Springer London, London, **2014**. ISBN 978-1-4471-6584-2. doi:10.1007/978-1-4471-6584-2_7.

[51] Paul L. Nunez, Ramesh Srinivasan, Andrew F. Westdorp, Ranjith S. Wijesinghe, Don M. Tucker, Richard B. Silberstein, and Peter J. Cadusch. Eeg coherency: I: statistics, reference electrode, volume conduction, laplacians, cortical imaging, and interpretation at multiple scales. *Electroencephalography and Clinical Neurophysiology*, 103(5):499 – 515, **1997**. ISSN 0013-4694. doi:https://doi.org/10.1016/S0013-4694(97)00066-7.

[52] Arnaud Delorme and Scott Makeig. Eeglab: an open source toolbox for analysis of single-trial eeg dynamics including independent component analysis. *Journal of neuroscience methods*, 134(1):9–21, **2004**.

[53] Andrew J. Parker. Binocular depth perception and the cerebral cortex. *Nature Reviews Neuroscience*, 8(5):379–391, **2007**. ISSN 1471-0048. doi:10.1038/nrn2131.

[54] H. Ramoser, J. Muller-Gerking, and G. Pfurtscheller. Optimal spatial filtering of single trial eeg during imagined hand movement. *IEEE Transactions on Rehabilitation Engineering*, 8(4):441–446, **2000**. ISSN 1558-0024. doi: 10.1109/86.895946.

[55] Michael Tangermann, Klaus-Robert Müller, Ad Aertsen, Niels Birbaumer, Christoph Braun, Clemens Brunner, Robert Leeb, Carsten Mehring, Kai Miller, Gernot Mueller-Putz, Guido Nolte, Gert Pfurtscheller, Hubert Preissl, Gerwin Schalk, Alois Schlögl, Carmen Vidaurre, Stephan Waldert, and Benjamin Blankertz. Review of the bci competition iv. *Frontiers in Neuroscience*, 6:55, **2012**. ISSN 1662-453X. doi:10.3389/fnins.2012.00055.

[56] Diederik P. Kingma and Jimmy Ba. Adam: A method for stochastic optimization, **2014**.

[57] Martín Abadi, Ashish Agarwal, Paul Barham, Eugene Brevdo, Zhifeng Chen, Craig Citro, Greg S. Corrado, Andy Davis, Jeffrey Dean, Matthieu Devin, Sanjay Ghemawat, Ian Goodfellow, Andrew Harp, Geoffrey Irving, Michael Isard, Yangqing Jia, Rafal Jozefowicz, Lukasz Kaiser, Manjunath Kudlur, Josh Levenberg, Dandelion Mané, Rajat Monga, Sherry Moore, Derek Murray, Chris Olah, Mike Schuster, Jonathon Shlens, Benoit Steiner, Ilya Sutskever, Kunal Talwar, Paul Tucker, Vincent Vanhoucke, Vijay Vasudevan, Fernanda Viégas, Oriol Vinyals, Pete Warden, Martin Wattenberg, Martin Wicke, Yuan Yu, and Xiaoqiang Zheng. TensorFlow: Large-scale machine learning on heterogeneous systems, **2015**. Software available from tensorflow.org.

[58] Francois Chollet et al. Keras, **2015**.

[59] Shang-Wen Chuang, Chun-Hsiang Chuang, Yi-Hsin Yu, Jung-Tai King, and Chin-Teng Lin. Eeg alpha and gamma modulators mediate motion sickness-related spectral responses. *International journal of neural systems*, 26(2):1650007, **2016**. ISSN 0129-0657. doi:10.1142/s0129065716500076.

[60] Khaitami, A. D. Wibawa, S. Mardi, S. Nugroho, and A. Z. Khoirunnisaa. Eeg visualization for cybersickness detection during playing 3d video games. In *2019 International Seminar on Intelligent Technology and Its Applications (ISITIA)*, pages 325–330. **2019**. ISSN null. doi:10.1109/ISITIA.2019.8937083.

[61] JASP Team. JASP (Version 0.11.1)[Computer software], **2019**.